Spring 5-18-2012

Pattern Recognition of Power System Voltage Stability using Statistical and Algorithmic Methods

Varun Togiti
vtogiti@uno.edu

Pattern Recognition of Power System Voltage Stability using
Statistical and Algorithmic Methods

A Thesis

Submitted to Graduate Faculty of the
University of New Orleans
in partial fulfillment of the
requirements for the degree of

Master of Science
In
Engineering
Electrical

By

Varun Kumar Togiti

B. E. Osmania University, 2009

May, 2012

To My Mother: Leelavathi

Acknowledgement

I would like to express my deepest gratitude to my academic and research advisor, Dr. Parviz Rastgoufard for his guidance and constant support in helping me to conduct and complete this work. His firm grasps and forte on all diverse areas of power systems ensured a steady stream of ideas and inspired me in every stage of this work. He has been a great source of inspiration and I am his student forever.

I would also like to express my appreciation to the members of my committee Dr. Ittiphong Leevongwat, and Dr. Dimitrios Charalampidis for all their support and useful feedback during my research. I would like to thank Entergy-UNO Power and Energy Research Laboratory for providing appropriate tools to finish this task.

I specially thank Nagendrakumar Beeravolu, for his valuable ideas and continuous guidance throughout this work.

Last but not least, I would like to thank my family and all my friends without whose support, this work would not be possible.

Table of Contents

List of Figures vii

List of Tables viii

Abstract ix

1 Introduction 1

1.1 Modern Power Systems 1

1.2 Power System Stability 2

1.3 Voltage Stability of Power System 3

1.4 A Review on Voltage Stability Analysis 6

1.5 Pattern Recognition 10

1.6 A Review on Pattern Recognition in Power Systems 13

1.7 Historical Review on Major Blackouts 15

1.8 Scope of Work 17

2 Mathematical Modeling 19

2.1 Power System Stability 19

2.2 Rotor Angle Stability 19

2.2.1 Transient Stability Analysis 22

2.2.2 Equal – area criterion 24

2.2.3 Numerical Integration Techniques 26

2.2.4 Direct Method of Transient Stability Analysis – Transient Energy Function Approach 27

2.3 Voltage Stability 29

2.4 Voltage Stability Analysis 32

2.4.1 Dynamic Analysis 33

2.4.2 Static Analysis 34

2.4.3 V-Q sensitivity analysis 35

2.4.4 Q-V modal analysis 36

2.5 Pattern Recognition 37

2.5.1 Regularized Least Squares classification (RLSC) 37

2.5.2 Data Mining – Classification and Regression Trees (CART) 39

3 Power System Models for Simulation 43

3.1 Introduction 43

3.2 Power System Simulator for Engineering (PSSE) 43

3.2.1 Generator Model 44

3.2.2 Excitation System Model 47

3.2.3 Maximum Excitation Limiter Model 48

3.2.4 Turbine Governor System Model 49

3.2.5 Power System Stabilizer Model 50

4 Test System 52

4.1 IEEE 39 Bus System 52

4.2 Bus Data 53

4.3 Generation Data 54

4.4 Load Data 55

4.5 Branch and Transformer data 56

4.6 Excitation System and Maximum Excitation Limiter data 58

4.7 Turbine Governor Model data 59

5 Research Simulations and Results 60

5.1 Simulations in PSS®E 60

5.2 Regularized Least Squares Method 65

5.3 CART 65

5.3.1 Feature 1 66

5.3.2 Feature 2 67

5.3.3 Feature 3 68

5.3.4 CART TREES 68

6 Summary and Future Work 71

6.1 Summary 71

6.2 Future Work 72

Bibliography 73

Vita 78

List of Figures

Simple power system model 20
Power - angle curve 21
Single - machine infinite bus system 22
Equivalent Circuit 23
Response to a step change in mechanical power input 24
A ball rolling on the inner surface of a bowl 27
Region of stability and its local approximation 28
A simple radial system for illustration of voltage stability phenomenon 30
Receiving end voltage, current and power as a function of load demand 31
The VR-PR characteristics of the system of Figure 2.8 32
$VR - QR$ characteristics of the system of Figure 2.8 with $PRPRMAX = 0.5$ 33
Classification Trees - After a successive sample partitions a classification decision is made at the terminal nodes 40
Generator model equivalent current source and Norton Equivalent Circuit 44
Electromagnetic Model of Round Rotor Generator (GENROU) 46
Rotating DC Exciter 47
ESDC1A excitation system model 47
Inverse Time characteristics of MAXEX1 48
Block Diagram of MAXEX1 49
IEEG3 hydro governor model 50
PSS2A Stabilizer Model 51
One line diagram of IEEE 39 bus system 52
Area chosen for voltage stability analysis 61
Voltage magnitude of Training case 3 - stable 63
Voltage magnitude of Training Case 12 – Unstable 64
Feature 1 66
Feature 2 67
CART Tree obtained for training data using Feature 1 69

LIST OF TABLES

Table 2-1 Learning sample matrix with n attributes and m measurement vectors 40

Table 3-1 Reactances and Time Constants used for modeling 45

Table 4-1 IEEE 39 Bus, bus data 53

Table 4-2 IEEE 39 Bus, Generation data 54

Table 4-3 Generator Dynamics data 55

Table 4-4 IEEE 39 Bus, Load data 55

Table 4-5 IEEE 39 Bus, Branch data 56

Table 4-6 IEEE 39 Bus, Transformer data 57

Table 4-7 Excitation System data 58

Table 4-8 Maximum Excitation Limiter Model data 58

Table 4-9 Turbine Governor Model data 59

Table 4-10 Turbine Governor Model data (2) 59

Table 5-1 Training cases 62

Table 5-2 Testing cases 64

Table 5-3 Results from RLSC algorithm 65

Table 5-4 Feature 1 and data input format to CART 66

Table 5-5 Data format for feature 2 67

Table 5-6 Data input format for feature 3 68

Table 5-7 Data input format for CART 68

Table 5-8 CART output for testing cases 69

Table 5-9 Results from CART 69

ABSTRACT

In recent years, power demands around the world and particularly in North America increased rapidly due to increase in customer's demand, while the development in transmission system is rather slow. This stresses the present transmission system and voltage stability becomes an important issue in this regard. Pattern recognition in conjunction with voltage stability analysis could be an effective tool to solve this problem

In this thesis, a methodology to detect the voltage stability ahead of time is presented. Dynamic simulation software PSS/E is used to simulate voltage stable and unstable cases, these cases are used to train and test the pattern recognition algorithms. Statistical and algorithmic pattern recognition methods are used. The proposed method is tested on IEEE 39 bus system. Finally, the pattern recognition models to predict the voltage stability of the system are developed.

KEYWORDS: Voltage stability, Pattern Recognition, Blackout, RLSC, CART, PSSE.

Chapter 1

1 INTRODUCTION

The purpose of this introductory chapter is to provide a general description of modern power systems, its stability and voltage stability in particular. Different kinds of pattern recognition techniques currently used are presented, particularly focusing on statistical and algorithmic approaches. A historical review of the voltage stability problem and the pattern recognition methods is presented. Finally, the outline of this thesis is explained.

1.1 MODERN POWER SYSTEMS

The commercial use of electricity began in the late 1870s when arc lamps were used for lighthouse illumination and street lighting [1]. The first complete electric power system (comprising of generator, cable, fuse, meter, and loads) was built by Thomas Edison- the historic Pearl Street Station in New York City which began operation in September 1882. With development of motors by Frank Sprague in 1884, motor loads were added to the systems.

These initial systems were dc (direct current). Eventually, ac (alternating current) systems dominated the dc systems for the following reasons:

- Voltage levels can be easily transformed in ac systems.
- AC generators are much simpler than dc generators.
- AC motors are much simpler and cheaper than dc motors.

In early period of ac power transmission, frequency was not standardized. In order to facilitate the interconnection of different grids, 60 Hz was adopted as standard.

The increasing need for transmitting larger amounts of power over longer distances created an incentive to use progressively higher voltage levels. To avoid the proliferation of an unlimited number of voltages, the industry has standardized voltage levels. The standards are 115, 138, 230 kV for the high voltage (HV) class, and 345, 500 and 765 kV for the (EHV) class [1].

Interconnection of neighboring utilities usually leads to improved system security and economy of operation. Almost all the utilities in the United States and Canada are now part of one interconnected system. This results in a very large system of enormous complexity. The design of such a system and its secure operation are indeed challenging problems.

In recent years, power demands around the world generally and particularly in North America will experience rapid increases due to the increase of customers' requirements. The report from Renewable Energy Transmission Company (RETCO) [2] about the infrastructure situation of U.S. electric grids states that electricity consumption accounts for 40% of all energy consumed in the U.S. and the electricity demand grows significantly and it will reach an increase rate of 26% by 2030.

Since 1982, growth in peak demand for electricity has exceeded transmission growth by almost 25% every year. Yet spending on research and development is the lowest of all industries [3]. Even with increase in demand, there has been chronic underinvestment in getting energy where it needs to go through transmission and distribution which limits grid efficiency and reliability. Since 2000, only 668 additional miles of interstate transmission have been built [3]. As a result, system constraints worsen at a time when outages and power quality issues are estimated to cost American business more than $100 billion on average each year. Under these extreme conditions, the need for maintaining stable operation of the grid is most important.

1.2 POWER SYSTEM STABILITY

"Power system stability is the ability of an electric power system, for a given initial operating condition, to regain a state of operating equilibrium after being subjected to a physical disturbance, with most system variables bounded so that practically the entire system remains intact" [4]. This definition applies to an interconnected power system as a whole. The stability of a particular generator or a group of generators is of interest. A remote generator may lose synchronism without causing cascading instability of the whole system. Similarly, stability of particular loads or load areas may be of interest.

The power system is a highly non-linear system due to the constantly changing loads, generator outputs and key operating parameters. When subjected to a disturbance, the stability of the power system depends on the initial operating conditions and the type of disturbance occurred. Power systems are subjected to a wide range of disturbances, small and large. Small disturbances such as changes in residential loads occur continuously; the system must be able to withstand these disturbances and operate in equilibrium condition. Large disturbances such as a short circuit on a transmission line or loss of a large generating unit may also occur. These disturbances may change topology of the system due to the isolation of faulted elements.

The power system in general is not designed to withstand all possible large disturbances possible because it is impractical and uneconomical [4]. The disturbances which have high probability of occurrence are chose while designing a contingency to study its mitigating process. A stable equilibrium set thus has a finite region of attraction; the larger the region, the more robust the system with respect to large disturbances.

Power system stability is a single problem; but in order to deal with different types of instabilities occurring in the system and study them effectively, we cannot treat it such. Because of high dimensionality and complexity of stability problem, it helps to make simplifying assumptions to analyze specific types of problems using an appropriate degree of detail of system representation and appropriate analytical techniques. The understanding of stability problems is greatly facilitated by the classification of stability into various categories [1]. The power system stability is mainly divided into rotor angle stability, frequency stability and voltage stability. Voltage stability problem is explained in detail as it is the main focus of this thesis.

1.3 VOLTAGE STABILITY OF POWER SYSTEM

Voltage stability is the ability of the power system to maintain steady acceptable voltages at all the buses in the system under normal operating conditions and after being subjected to a disturbance [1]. Voltage instability occurs when a disturbance, increase in load demand or change in system condition causes a progressive and uncontrolled drop in voltage. The main factor causing instability is the inability of the power system to meet the reactive power demand. A possible outcome of voltage instability is loss of load in an area, or tripping of transmission lines and other elements by their protective systems leading to cascading outages. Voltage collapse is the process by which the sequence of events accompanying voltage instability leads to a blackout or abnormally low voltages in a significant part of the power system.

The voltage instability is mainly caused because of the loads; after a disturbance, power consumed by the loads tends to be restored by the action of voltage regulators, tap changing transformers, and thermostats. Restored loads increase the stress on high voltage network by increasing the reactive power consumption and causing further voltage reduction. A run-down situation causing voltage instability occurs when load dynamics attempt to restore power consumption beyond the capability of transmission network and the connected generation [1], [5].

There is also a risk of overvoltage instability in the system which has been experienced at least once [6]. This is caused by the capacitive behavior of the network as well as by under excitation limiters preventing generators and/or synchronous compensators from absorbing the excess reactive power. This instability is associated with instability of the combined generation and transmission system to operate below some load level.

Voltage stability problems may also be experienced at HVDC links [7]. They are usually associated with HVDC links connected to weak ac systems and may occur at rectifier or inverter stations, and are associated with the unfavorable reactive power “load” characteristics of the converters. The HVDC link control strategies have a significant influence on such problems, since the active and reactive power at the ac/dc junction are determined by the controls. If the resulting loading on the ac transmission stresses it beyond its capability, voltage instability occurs. Such a phenomenon is relatively with the time frame of interest being in order of one second or less.

It is useful to classify voltage stability into sub categories as discussed below:

- *Large - disturbance Voltage Stability* is the ability of the system to maintain steady permissible voltages following large disturbances such as system faults, generator trips or other circuit contingencies. This phenomenon is affected by the system and load characteristics, and the interactions of both continuous and discrete controls and protections. Determination of large signal voltage stability requires the examination of the nonlinear response of the power system over a period of time sufficient to capture the performance and interactions of devices such as motors, under load tap changers, generator field current limiters, and speed governors. The study period of interest may extend from a few seconds to tens of minutes. Therefore, long-term dynamic simulations are required for analysis

- *Small – disturbance voltage stability* is the ability of the power system to maintain steady permissible voltages when subjected to small perturbations such as incremental changes in system load. This form of stability is influenced by the characteristics of the load, continuous controls, and discrete controls at a given instant of time. This concept is useful in determining, at any instant, how the system responds to small system changes. To identify the factors influencing stability, system equations can be linearized for the analysis with appropriate assumptions.

The time frame of interest for voltage stability problems may vary from a few seconds to tens of minutes. Therefore, voltage stability can be classified into short term and long term on this basis.

- *Short – term voltage stability* involves dynamics of fast acting load components such as induction motors, electronically controlled loads, and HVDC converters. The study period of interest is in order of several seconds, and the analysis requires solution of appropriate system differential equations [4]. This analysis needs dynamic modeling of loads.
- *Long – term voltage stability* involves slower acting equipment such as tap-changing transformers, thermostatically controlled loads, and generator current limiters. This analysis assumes that inter – machine synchronizing power oscillations have dumped out, resulting in a uniform system frequency [8]. The focus is on slower and longer duration phenomena that accompany large scale system upsets and on the resulting large, sustained mismatches between the generation and consumption of active and reactive powers. Long – term stability is usually concerned with system disturbances that involve contingencies beyond the normal system design criteria.

1.4 A REVIEW ON VOLTAGE STABILITY ANALYSIS

Voltage stability problems mainly occur when the system is heavily stressed beyond its capability. While the disturbance leading to voltage collapse may be initiated by a variety of causes, the main problem is the inherent weakness in the power system. The main factors other than strength of transmission network, power transfer capability are generator reactive power/voltage control limits, load characteristics, characteristics of reactive compensation devices, and the action of voltage control devices such as under load tap changing transformers (ULTCs) [1].

The voltage stability analysis for a given system state involves the examination of two concepts [9]:

a) *Proximity to voltage instability:* A measure of how close the system is to voltage instability? Physical quantities such as load levels, active power flow through critical interface and reactive power reserve can be used to measure the distance to instability. The most appropriate measure for a given situation depends on the specific system and the intended use of the margin. Considerations must be given to possible contingencies such as line outages, loss of generating units or reactive power sources, etc.
b) *Mechanism of voltage instability:* This includes the determination of the cause of instability including the key factors, voltage - weak areas and also finding out the measures to improve stability.

The voltage instability problem is solved by many different methods, which can be distinguished mainly into two groups: static and dynamic methods. Dynamic methods apply real – time simulation in time domain using precise dynamic models for all instruments in a power system. It shows the time domain events and their characteristic curves which eventually lead the system into voltage collapse. These methods mainly depend on the solutions of large sets of differential equations created to describe the model characteristics of electrical devices and their internal connections. Dynamic simulation is particularly effective for detailed study of specific voltage collapse situations and coordination of protection and time dependent action of controls. The dynamic simulation of large-scale power systems is time consuming and relies heavily on the computer's performance.

The system dynamics influencing voltage instability are usually slow. Therefore, static methods can be used to analyze many aspects of the problem. The static analysis techniques allow examination of a wide range of system conditions and, if appropriately used, can provide much insight into the nature of the problem and identify the key contributing factors.

The electric utility has been largely dependent on conventional power-flow programs for static analysis of voltage stability. Stability is determined by generating V-P and Q-V curves at selected load buses. These curves are generated by executing a large number of power flows which is usually time consuming. These procedures focus on individual buses, that is, the stability is studied by stressing a particular bus in the system. This may unrealistically distort the stability of the system.

F. D. Galiana used load flow feasibility to indicate proximity to voltage collapse [10]. The feasibility region (FR) is defined as the set of generalized bus injections (P, Q, or V^2 at each bus) for which a load flow exists. The feasibility margin is a scalar ranging between 0 and 1 which measures the proximity of a bus injection vector to the boundary of FR. This method does not rely on the load flow or optimal load flow simulations. Feasibility limit is to be defined from experience and then by monitoring a distance measure form this limit, one can monitor the voltage collapse condition.

V-Q sensitivity analysis has advantage that it provides voltage stability-related information from a system-wide perspective and clearly identifies areas that have potential problems [1].This method uses the conventional linearized power flow model. The elements of the Jacobian matrix give the sensitivity between power flow and bus voltage changes. The Jacobian matrix is reduced in size by considering P (real power) to be constant at each operating point. The V-Q sensitivity at a bus represents the slope of the Q-V curve at the given operating point. A positive V-Q sensitivity is indicative of stable operation; the smaller the sensitivity, the more stable the system. As stability decreases, the magnitude of sensitivity increases, becoming infinity at the stability limit. A negative sensitivity is indicative of unstable operation. A very small negative value indicates a very unstable operation.

B. Gao, G. K. Morison, P. Kundur presented a voltage stability assessment technique for large power systems using modal analysis [9]. This method computes a specified number of smallest eigen values of a reduced Jacobian matrix (considering voltage and reactive power), and the associated bus, branch and generation participation factors. Each eigen value corresponds to a mode of voltage/reactive power variation and gives information about that mode. The small eigen values represent the modes most prone to loss of stability. The magnitude of each small eigen value provides a relative measure of proximity to loss of voltage stability for that mode. Bus, branch and generator participation factors provide useful information regarding the mechanism of loss of stability. This gives an insight of the system and helps in taking remedial actions to prevent the voltage collapse.

The load flow Jacobian and its properties are used to study the voltage instability [11] [12] [13]. The relationship between multiple load flow solutions and voltage instability has been studied by Y. Tamura, ET. Al. [11]. Under heavy – conditions, multiple load flow solutions are likely to appear. The authors suggest analyzing static and/or semi – dynamic performance of the problem and then the relationship between the dynamic factors and voltage instability. They assume that one is stable and the other is unstable if there is a pair of multiple load flow solution. Then a sequence of criteria is applied to the individual members of the solution pair to see their difference in behavior. Three criteria are used, the sign of Jacobian determinant in the load flow calculations, load flow sensitivity for load injections and system parameters, and stored energy of the elements L and C in the electric power system. For a stable operating condition, the sign of determinant of the Jacobian matrix is determined. Then as the system operating condition changes, for each condition, the sign of the determinant of the Jacobian is compared with the one determined earlier (for stable operating point). If the signs are equal, the system is assumed to be stable, if not unstable. This method has some uncertainty and this cannot be used as a standalone representation of instability. This method when used in conjunction with the other two criteria discussed above, can be used to determine the instability in power systems.

The singular value decomposition of Jacobian matrix is used to come up with voltage stability indices [13]. The sub-matrices of the Jacobian are used as static voltage stability indicators. The sub-matrices are obtained by setting the real power constant in the power flow equation. The value of the smallest singular value gives a measure of the proximity to the steady state voltage stability limit. This method allows more realistic modeling of power systems equipment such as voltage dependent voltage dependent loads, generator reactive limits, etc. Li

– Jun Cai, and Istvan Erlich proposed a novel approach which includes all possible active and reactive power controls based on the multi-input multi-output transfer (MIMO) function and singular value decomposition (SVD) [14]. As seen in the above discussed approaches, the classical methods consider the active powers at all buses as constant. Voltage stability control methods such as reactive power compensation, under voltage load shedding, and transformer tap changers can also be taken into consideration using this method. These controls are selected as inputs to the MIMO system. The incremental changes in the bus voltage magnitudes are considered as the output variables. The input singular vectors are used to select the most suitable control signal for the improvement of steady state voltage stability and the output singular vectors provide an overview of the most critical buses that are affected by the static voltage stability. Since the inputs and outputs of the real system can be restricted to a small range, this method can also be applied to large power system networks.

Though static voltage stability analysis is used extensively in the power industry, there are some restrictions on this approach. The classic methods are mostly based on modal analysis, which requires the number of inputs (reactive power changes) be equal to the number of outputs (voltage magnitude changes). In large power systems, there may be additional controls which need to be included in the input. Only the effect of PQ-bus reactive power is considered, while in practice, the active power changes also have great influence on the static voltage stability. The effect of automatic voltage regulators (AVRs) cannot be included in the classic analysis [14].

Dynamic simulation accurately includes the time dependent actions of control and protection. Modeling for dynamics include more detailed representation of loads and all other equipment in power systems. Enormous increase in computing capacity has enabled us to use the dynamic simulations to analyze voltage stability problem. It still is a time consuming process, but a compromise between accuracy and speed by using other techniques is the fast dynamics [15]. A review on use of dynamic simulations for voltage stability analysis is presented below.

M.H.Haque and U.M.R.Pothula investigated the dynamic aspect of voltage stability problem of a simple power system by considering the dynamic effect of both fast acting and slow acting devices [16]. Based on time scale of operation, voltage stability can be classified into short-term, mid-term and long-term [1]. In short-term, the dynamics of fast-acting devices, such as generators, induction motors, switched capacitors, etc. determine the system performance. In mid-term and long-term, the dynamics of slow acting devices such as transformer on-load tap changers (OLTC), generator over excitation limiters (OXL), etc., comes into play. Differential equations are used describe the dynamics of generators, OLTCs, OXLs, and loads. The effect of slow acting devices on long-term voltage stability is studied using MATLAB/SIMULINK.

J. H. Chow and A. Gebreselassie used eigen value analysis, sensitivity analysis, and nonlinear voltage simulations to study the dynamic phenomenon of voltage instability [17]. They analyzed a simple power system consisting of a single machine and a constant power load. Eigen value analysis approach is used to evaluate the effects of some of the control parameters on the voltage stability limits of the single machine system model. The eigenvalue analysis predicts the values of the system parameters for which, any small disturbance will initiate unstable voltage oscillations. ACSL (Advanced Continuous Simulation Language) is used to perform nonlinear simulation for the predicted system conditions and to investigate the effects of these oscillations. They have also determined the need for more detailed load, generation models to establish realistic stability properties.

M. Hasani and M. Parniani studied the voltage stability analysis using a method combining static and dynamic analysis [18]. Using static methods, a voltage stability ranking was performed to define faint buses, generators and links in terms of voltage stability. More detailed modeling was used to analyze the dynamics of most severe conditions. Many detailed dynamic analyses are done using more detailed modeling of loads and other equipment in power systems [19], [20]. T. X. Zhu, S. K. Tso, and K. L. Lo have investigated the effect of on-load tap changers on the maximum power transfer limit [21].

1.5 PATTERN RECOGNITION

By the time they are five years old, most children can recognize digits and letters. Small characters, large characters, handwritten, machine printed are easily recognized by young. We take this ability for granted. “Pattern recognition is the study of how machines can observe the environment, learn to distinguish patterns of interest from their background, and make sound and reasonable decisions about the categories of the pattern” [22]. Automatic (machine) recognition, description, classification, grouping of patterns are important problems in a variety of engineering and scientific disciplines such as biology, psychology, medicine, marketing, computer vision, artificial intelligence, and remote sensing. This technique is being implemented in power systems field to develop tools which can take decisions automatically regarding various issues [23], [24,24], [25].

A pattern could be a fingerprint image, a handwritten cursive word, a human face or a speech signal. Given a pattern, its recognition/classification may consist of one of the following two tasks: 1) supervised classification in which the pattern is identified as a member of predefined class, 2) unsupervised classification in which the pattern is assigned to a hitherto unknown class. Here the recognition problem is posed as a classification or categorization task, where the classes are defined by the system designer (in supervised classification) or are learned based on the similarity of patterns (in unsupervised classification).

The rapid development of computing power, which enables fast processing of huge data sets, has also facilitated the use of elaborate and diverse methods of classification. The data being collected in every field is enormously increasing, such as P.M.U (Phasor Measurement Unit) data in the power industry. This creates a demand for automatic pattern recognition systems and also stringent performance requirements (speed, accuracy, and cost). In this development of process, no single recognition technique is “optimal”, so multiple methods and approaches have to be used.

The design of pattern recognition system essentially involves the following three aspects: 1) data acquisition and preprocessing, 2) data representation (features), and 3) decision making. Learning from a set of examples (training set) is an important and desired attribute of most pattern recognition techniques. Various types of pattern recognition techniques are discussed below:

- ***Statistical Approach:*** In statistical approach, each pattern is represented in terms of d features or measurements and is viewed as point in d - dimensional space. The goal is to choose those features that allow pattern vectors belonging to different categories to occupy compact and disjoint regions in a d-dimensional feature space. The effectiveness of the representation space (feature set) is determined by how well patterns from different classes can be separated. Given a set of training patterns from each class, the objective is to establish decision boundaries in the feature space which separate patterns belonging to different classes. A disadvantage of this approach is that too much statistical information or unavailable statistical information may be needed for the solution.

- ***Syntactic Approach:*** In this approach, a pattern is viewed as being composed of simple subpatterns which are yet themselves built from yet simpler subpatterns [22]. The simplest/elementary subpatterns to be recognized are called *primitives* and the given complex pattern is represented in terms of the interrelationships between these primitives. In syntactic pattern recognition, a formal analogy is drawn between the structure of patterns and the syntax of a language. The patterns are viewed as sentences belonging to a language, primitives are viewed as the alphabets of the language, and the sentences are generated according to a grammar. Thus a large number of complex patterns can be described by a small number of primitives and grammatical rules. The grammar for each pattern class must be inferred from the available training samples. The implementation of this technique leads to difficulties which primarily have to do with the segmentation of noisy pattern (to detect the primitives) and the interference of the grammar from training set.
- ***Neural Networks:*** Neural networks can be viewed as massively parallel computing systems consisting of an extremely large number of simple processors with many interconnections. Neural network models attempt to use some organizational principles (such as learning, generalization, and computation) in a network of weighted graphs in which the nodes are artificial neurons and directed edges (with weights) are connections between neuron outputs and inputs. The main characteristics of neural networks are that they have ability to learn complex nonlinear input – output relationships, use sequential training procedures, and adapt themselves to the data. A main disadvantage of the neural network approach is that it may take considerable computer time and memory. Another disadvantage is that we may not have enough representative training samples that would allow the solution to provide the necessary generalization to non-training patterns.

I have used CART (Classification and Regression Trees) which is a statistical pattern recognition technique and RLSC (Regularized Least Squares Classification) which is neural network approach. These techniques are discussed in detail in chapter 3.

1.6 A REVIEW ON PATTERN RECOGNITION IN POWER SYSTEMS

Pattern recognition is being widely used in several fields of engineering and sciences including power systems. There have been many literatures on the use of pattern recognition for transient, dynamic stability assessment, controlled islanding, and many other applications in power systems, [23] , [24], [25].

L. S. Moulin, et al., applied support vector machines (SVM), a recently introduced learning – based nonlinear classifier approach to analyze transient stability analysis (TSA) in power systems [24]. Power systems analysis is enormously high dimensional problem, and this makes pattern recognition technique a promising tool for the analysis. The integration of automatic learning/pattern recognition techniques with analytical TSA methods can provide more accurate monitoring, fast decision making, etc.,. It also avoids the repetitive burden of analyzing similar operating points. Neural networks (NNs) technology has been reported as an important contributor for reaching the goals of online TSA [26]. Support vector machines (SVM) rely on support vectors (SVs) to identify the decision boundaries between different classes. SVMs can map complex nonlinear input/output relationships, and are well suited for TSA because our focus is on the boundary between stable and unstable operating points. Instead of using entire data available, features are extracted from it, and are used for pattern recognition. Feature selection reduces the input dimensionality in order to use as few variables as possible, getting a more concise representation of power system.

An SVM classifier minimizes the generalization error by optimizing the tradeoff between the number of training errors and the so-called Vapnik – Chervonenkis (VC) dimension, which is a new concept of complexity measure. The SVMs employed for two-class problems are based on hyper planes to separate the data in an n-dimensional space. The hyper plane that maximizes margin of separation between the two classes is intuitively expected to have better generalization ability. This technique has been tested on a subsystem of the Brazilian Southeast grid. For each transient stability analysis, a major branch is assumed to be under scheduled maintenance and single contingencies are assumed for the remaining branches. These cases are simulated in the time-domain, and each one is classified as stable or unstable. As expected, the stable cases outnumber the unstable cases in any analysis. This difference can affect the performance of SVM; this problem is dealt by artificially decreasing the number of stable cases and using equal number of stable and unstable cases. The active and reactive power at the relevant buses is chose for training and the classifier is either stable (+1) or unstable (-1). The following conclusions are drawn [24]:

- SVMs fit the TSA task for large power systems
- SVMs performed better when complete data set was used (which include more stable cases)
- There have been some false dismissals (unstable cases classified as stable, which is extremely undesirable)
- The stability studies database already available at the utilities can be used with NN-based TSA.

A hybrid approach based on direct-type methods coupled with detailed time simulation is considered as a promising idea for TSA of large – scale power systems. The NNs can be used as filters to discard stable contingencies in a very fast way [27].

Peng Zhang and Jing Peng have studied the performance of support vector machines (SVMs) and regularized least squares (RLS) by applying both the techniques to a collection of data sets [28]. As discussed earlier, SVMs realize the structure risk minimization principle by maximizing the margin between the separating plane and the data. The regularized least squares (RLS) method constructs classifiers by minimizing a regularized functional directly in a reproducing kernel Hilbert space. The SVM solution produces a hyper plane having the maximum margin between different classes of data. Regarding complexity of solution, the computational cost associated with SVM is incurred by solving a quadratic programing problem. On the other hand, for RLS, linear system of equations is needed to be solved, which is less complex. Two methods are used with both real and simulated data. The performance of both methods is almost similar. The RLS methodology is strikingly simple. On the other hand, SVMs have a compact representation of solutions, which may be important in time – critical applications.

Decision trees (a statistical pattern recognition approach) have been used to analyze the stability, security and stable operation of power systems [29], [23], and [30]. Ruisheng Diao, et al., have developed an online voltage security assessment scheme using synchronized Phasor measurements and periodically updated decision trees (DTs) [29]. Phasor measurement units (PMUs) utilize the global positioning system (GPS) receivers and microprocessors to monitor the state of the power system; they are very accurate and fast. The time-stamped digital phasors calculated in the PMUs are synchronized to a common time frame by satellites and then assembled into a series of data streams for communication to remote control centers. The created database consists of different cases that are represented by a vector of predictors and an objective (for example secure or insecure state), a DT is designed for successful classification of this objective by using only a small number of these predictors. A number of pre-disturbance operating conditions (OC) for the past representative data and the forecasted ones for the next 24 hours are collected a day ahead. Detailed voltage security analysis is conducted for all these operating conditions for critical contingencies, and each contingency case at different OCs is then assigned a voltage security label. This can be either secure or insecure. By collecting PMU related system parameters, DTs are trained offline to obtain security classifications for next day. These DTs are updated on hourly basis, if there are any major changes in the system topology. The updated DTs are then used for online applications for next hour. Measurements from PMUs are continuously collected in real time and decision trees are used to assess the system condition. Decision trees can be combined with other data mining tools like support vector machine and random forests to pursue better prediction accuracy.

1.7 HISTORICAL REVIEW ON MAJOR BLACKOUTS

In the last decade, several major blackouts were reported in several research papers [31], [32], [33]. Deregulation was introduced to improve the managerial efficiency of power systems as its size and the load demand increased enormously. This created a competitive market structure, and increased the system utilization. This also increased the risk on system operations by stressing the power systems and reducing the predictability of operations [31]. Usually, a power system is designed for N-1 contingencies, but is still not enough to secure the system. The review of major blackouts will give the system designers an overview of the problems underneath and the mitigating steps to be taken in future.

The first massive power failure properly reported was the Northeast power failure on 9th November 1965 in the United States. The weak transmission line between northeast and southwest was the main cause. At heavy loading conditions, the backup protection tripped one out of five transmission lines. This is because the relay was set to low load level. Thus the other four lines were also successively tripped, diverting 1700 MW of power which overloaded several other lines and finally the system collapsed. It was identified that there was not enough spinning reserve at the time the blackout was initiated. Extra High Voltage transmission lines were proposed to be built, less essential load shedding was introduced, and keeping distributed spinning reserve was put into practice to avoid future collapses. This failure affected 30 million people; New York City was in darkness for 13 hours.

On 13th July 1977, there was a power failure due to the collapse of Con Edison system. The collapse resulted from a combination of natural events, equipment malfunctioning, questionable system design features and operating errors as lack of preparation for emergencies [34]. Severe thunderstorm and lightning strikes hit two lines; protective equipment of each line was imperfectly operated and resulted in three of the four lines tripping. Transmission ties increasingly overloaded for about 35 minutes and all ties were opened. After 6 minutes, the entire system was out of operation. This might have been easily prevented by a timely increasing of generation or manual load shedding. The system was instructed to operate well within the cautious interpretations of such severities. The research and development penetrated into the blackouts and more accurate modeling of the power system components was practiced.

A power failure occurred in Tokyo, Japan on 23rd July 1987 affecting 2.8 million customers with the outage of 3.4 GW power. The reserve was kept at 1.52 GW and it was sufficient to manage the usual demand increase. Unusual high peak demand due to extreme hot weather caused the failure. Increase in demand (400MW/minute) exceeded the expected level. This increasing demand gradually reduced the voltage of the 500 kV trunk network within 5 minutes to 460 kV. Constant power characteristic loads such as air conditioners reduced the network voltage rapidly and caused dynamic voltage instability. The system was recovered within 90 minutes. As future precautions, the operators increased the trunk line voltage by 5% of its normal operation during summer time. A 1 GW power plant was proposed to be built closer to the load center, and shunt capacitors together with SVC of 1,550 MVAR were installed.

The US Canadian blackout on 14th August 2003 affected about 50 million people, 63 GW load was interrupted. In this event, 400 transmission lines and 531 generating units at 261 power plants tripped. "Blackout was caused by deficiencies in specific practices, equipment, and human decisions by various organizations that affected conditions and outcomes that afternoon" [33]. The major reason was found to be insufficient reactive power, which leads to voltage instability. As the computer software systems were not operating properly, the operators were not warned in advance about the system condition. Failure initiated with a tripping voltage regulator due to over excitation and when the operators attempted to restore the regulators, generators tripped. These generators were generating high reactive power, which was continuously increasing as the day progressed. A 345 kV transmission line loaded with 44% tripped in 90 minutes due to tree contact. Another line loaded with 88% tripped at 128 minutes due to another tree touching. Finally critical failure made on a tie line 158 minutes later by a relay. The major tie line trip reversed the power flow and lead to cascading blackout of the entire region. The major tie line tripping might have been protected by load shedding.

According to the records of major disturbances, the system faults are cleared in milliseconds, then system fault transients remained for several seconds and blackouts occurred in several minutes. This show a scope, where if immediate actions were taken, the blackouts would have been prevented. Many research papers are being published on online voltage stability analysis techniques which could help prevent the blackouts.

1.8 SCOPE OF WORK

In this thesis, a pattern recognition approach to detect the voltage instability in a power system in advance to its occurrence is proposed. This could help the operators to take remedial actions, and thus prevent the oncoming voltage collapse phenomenon. A pattern recognition software, CART (Classification and Regression trees) and RLSC (Regularized Least Squares Classification) are used to develop the voltage stable and voltage unstable patterns. This is achieved by simulating voltage stable and unstable cases from a test system and then training the pattern recognition models to come up with patterns. These patterns are later validated by testing those using new cases which are not used for training. IEEE 39 bus system is used as test system, it is modeled in PSS/E (Power System Simulator for Engineering), and contingencies are applied to come up with the training and testing cases. MATLAB is used to develop RLSC algorithm and also to preprocess the data which is to be analyzed with CART. This methodology could be a useful online application for voltage stability analysis in power systems.

Chapter 2

2 MATHEMATICAL MODELING

Mathematical modeling of the power system stability problem and voltage stability problem in detail are discussed in this chapter. Different methods to analyze the instability phenomena are explained.

2.1 POWER SYSTEM STABILITY

As mentioned in chapter 1, power system stability is the ability of power system to remain in state of operating equilibrium under normal operating conditions and to regain an acceptable state of equilibrium after being subjected to a disturbance. The stability analysis of power systems is broadly classified into two types:

- Rotor Angle Stability
- Voltage Stability

These two stability problems and their analyses are explained below:

2.2 ROTOR ANGLE STABILITY

Rotor angle stability is the ability of interconnected synchronous machines of a power system to remain in synchronism [1]. This stability problem involves electromechanical oscillations inherent to the power systems. The variation of electrical power output of synchronous machines with respect to the oscillations of the rotors is the main factor affecting stability.

Synchronous machines are predominantly used for power generation in power systems. The synchronous machine consists of field and armature. The field is on the rotor and the armature on the stator. The field winding is excited by direct current. When this field is rotated by a turbine, it induces alternating voltages in the three phase armature windings of the stator whose frequency is dependent on the speed of rotor. When two or more synchronous machines are interconnected, the voltages and currents of all the machines must have the same frequency.

A rotating magnetic field is created due to the alternating currents flowing in the armature winding. The stator and rotor fields interact with each other to produce an electromechanical torque. Under normal conditions, the stator and rotor fields rotate at the same speed, with an angular separation between them depending on the electrical power output of the generator.

The relation between transfer power and the angular positions of the rotors of the interconnected machines is an important factor in deciding stability. Let us consider a simple power system model shown in Figure 2.1. The figure represents a generator feeding a synchronous motor through a transmission line having inductance $\boldsymbol{X_L}$ and negligible resistance and capacitance.

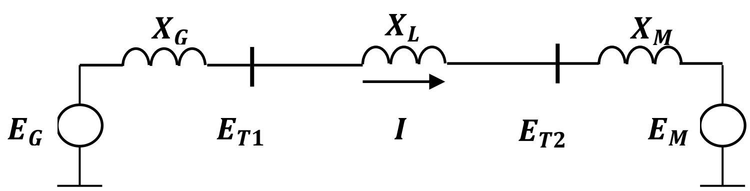

Figure 2.1 Simple power system model

A simple model comprising of voltage behind an effective reactance is used to represent synchronous machines. The power transferred from the generator to the motor is a function of angular separation (**δ**) between the rotors of the two machines. The power transferred from generator to motor is given by

$$P = \frac{E_G E_M}{X_T} \sin \delta \tag{2.1}$$

where

$X_T = X_G + X_L + X_M \; and \;\; \delta = \delta_G + \delta_L + \delta_M$

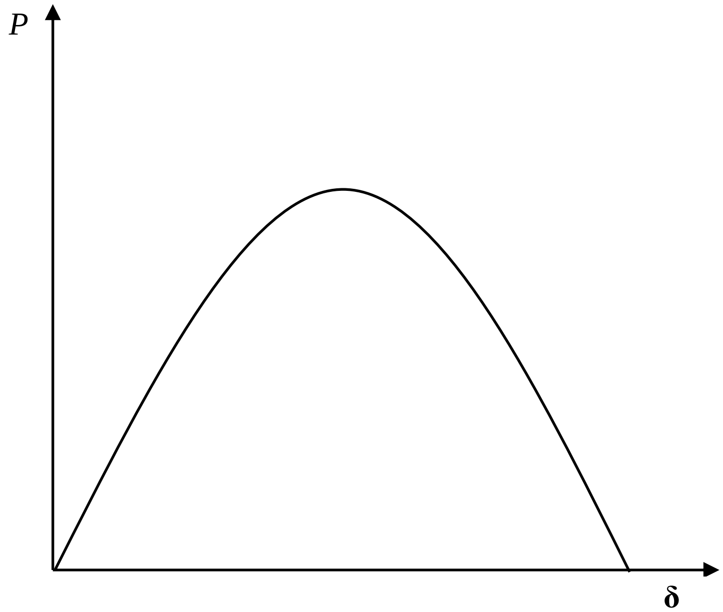

Figure 2.2 Power - angle curve

The power versus angle plot is shown in Figure 2.2. When the angle is zero, no power is transferred. As the angle increases, the power transferred increases up to a maximum. After a certain angle, nominally 90°, further increase in angle results in a decrease in power transferred. The magnitude of the maximum power transferred between two machines is directly proportional to the machine internal voltages and inversely proportional to the reactance between the voltages which include the reactance of the transmission line connecting the machines and the reactances of the machines. Stability is a condition of equilibrium between opposing forces in the power systems. Under normal operating conditions, there is equilibrium between the input mechanical and the output electrical torque of each machine and the speed remains constant. If the system is perturbed, this equilibrium is upset, resulting in acceleration or deceleration of the rotors of the generators according to the laws of motion. If one generator temporarily runs faster than the other, its angular position corresponding to the slower machine advances. The resulting angle transfers a part of load from slower machine to the faster machine as per the power – angle relationship. This tends to decrease the speed difference and thus the angular separation. If the angular separation increases beyond a certain limit, the power transfer decreases; which further increases the angular separation leading to instability.

In electric power systems, the change in electrical torque of a synchronous machine following a perturbation can be resolved into two components:

$$\Delta T_e = T_S \Delta\delta + T_D \Delta\omega \tag{2.2}$$

Where $T_S\Delta\delta$ is the component of torque change in phase with the rotor angle perturbation $\Delta\delta$ and is referred to as *synchronizing torque coefficient*. $T_D\Delta\omega$ is the component of torque in phase with the speed deviation $\Delta\omega$ and is referred to as *damping torque component*. Both synchronizing and damping torques are needed for stable operation of power systems. Lack of sufficient synchronizing torque results in instability through an *aperiodic drift* in rotor angle. On the other hand, lack of sufficient damping torque results in *oscillatory instability*.

The rotor angle stability is further categorized into small signal stability and transient stability.

- Small signal stability is the ability of power system to maintain synchronism under small disturbances which occur continually because of variations in loads and generations. The instability may arise due to insufficient synchronizing or damping torques.
- Transient stability is the ability of the power systems to maintain synchronism when subjected to severe transient disturbances such as a fault on transmission facilities, loss of generation or loss of a large load, etc. Stability depends on both the initial operating state of the system and is influenced by the nonlinear power - angle relationship.

2.2.1 Transient Stability Analysis

The nature of transient stability is explained here. In the system shown in Figure 2.3 [1], a generator is delivering power to a large system represented by an infinite bus through two transmission circuits. The system model is reduced to the form shown in Figure 2.4 .

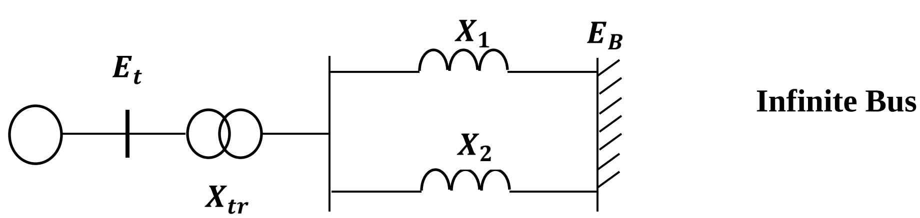

Figure 2.3 Single - machine infinite bus system

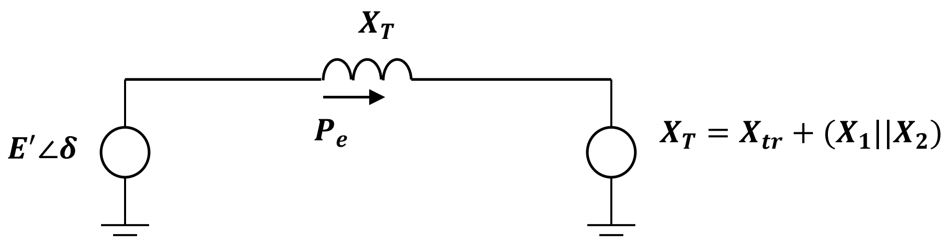

Figure 2.4 Equivalent Circuit

The generator's electrical output is

$$P_e = \frac{E' E_B}{X_T} \sin\delta = P_{max} \sin\delta \tag{2.3}$$

The equation of motion or the swing equation can be written as

$$\frac{2H}{\omega_o} \frac{d^2\delta}{dt^2} = P_m - P_{max} \sin\delta \tag{2.4}$$

Where P_m is the mechanical power input to the generator, H is the inertia constant, δ is the rotor angle and *t* is time in seconds.

The transient behavior of the system can be examined by considering a sudden increase in the mechanical input from P_{m0} to P_{m1} as shown in Figure 2.5 [1]. Because of inertia of the rotor, the rotor angle cannot change directly from δ_0 to δ_1 corresponding to the new equilibrium point *b* at which $P_e = P_{m1}$. As the mechanical power is more than the electrical output, the rotor accelerates from the initial point a to the point *b* tracing the $P_e - \delta$ curve according to the swing equation. At any instant, the difference between mechanical input P_m and electrical output P_e represents the accelerating power. When point *b* is reached, the accelerating power is zero but the rotor speed is higher than the synchronous speed ω_0(corresponding to the infinite bus). Hence, the rotor angle continues to increase. For values of δ higher thanδ_1, P_e is greater than P_{m1} and the rotor decelerates. At some peak value δ_m, the rotor speed recovers to the synchronous value ω_0, but P_e is higher than P_{m1} which causes the rotor to decelerate with the speed dropping

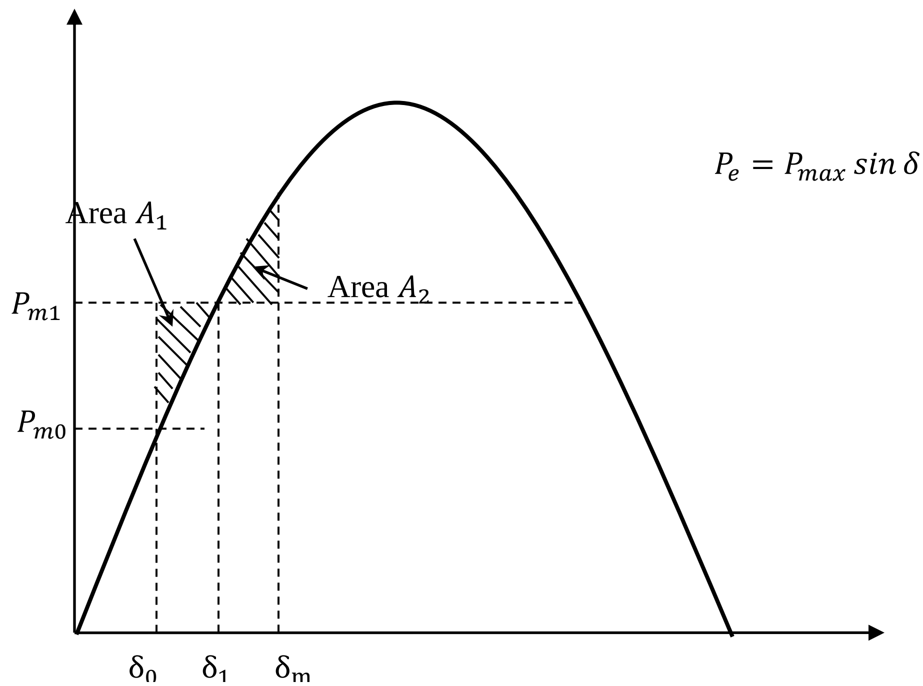

Figure 2.5 Response to a step change in mechanical power input

below ω_0; the operating point retraces the $P_e - \delta$ curve from c to b and then to a. The rotor angle oscillates indefinitely about the new equilibrium angle δ_1. If we consider all the resistances and the complete model of generator, many positive damping forces act on the rotor causing it to reach the new equilibrium point b.

2.2.2 EQUAL – AREA CRITERION

It is not necessary to solve the swing equation to find out whether the rotor angle increases indefinitely or settles at equilibrium point for disturbances. Using the power angle diagram shown in Figure 2.5, stability limits can be calculated. Rearranging and integrating (2.4) gives

$$\left[\frac{d\delta}{dt}\right]^2 = \int \frac{\omega_0(P_m - P_e)}{H} d\delta \tag{2.5}$$

The speed deviation $\boldsymbol{\frac{d\delta}{dt}}$ is initially zero. It will change as a disturbance occurs. For stable operation, the deviation of angle δ must reach a maximum value and then change direction. This requires $\boldsymbol{\frac{d\delta}{dt}}$ becoming zero after disturbance. The criterion for stability can be written as:

$$\int_{\delta_0}^{\delta_m} \frac{\omega_0}{H} (P_m - P_e) d\delta = 0 \tag{2.6}$$

Where $\boldsymbol{\delta_0}$ the initial rotor is angle and $\boldsymbol{\delta_m}$ is the maximum rotor angle as shown in Figure 2.5. The area under the function $\boldsymbol{P_m - P_e}$ plotted against δ must be zero if the system is to be stable. Kinetic energy is gained by the rotor during acceleration from $\boldsymbol{\delta_0}$ to $\boldsymbol{\delta_1}$. The energy gained is

$$E_1 = \int_{\delta_0}^{\delta_1} (P_m - P_e) d\delta = \ area\ A_1 \tag{2.7}$$

The energy lost during deceleration when δ changes from $\boldsymbol{\delta_1}$ to $\boldsymbol{\delta_m}$ is

$$E_2 = \int_{\delta_1}^{\delta_m} (P_e - P_m) d\delta = \ area\ A_2 \tag{2.8}$$

The stability is maintained only if an area A_2 at least equal to A_1can be located above P_{m1}.The criterion for stability can be stated as follows:

The system is stable if area $A_2 \geq A_1$ and unstable if $A_1 > A_2$. This technique can be extended to analyze the stability phenomenon for different types of faults in power systems.

2.2.3 NUMERICAL INTEGRATION TECHNIQUES

In time domain simulation, which is the most practical method of transient stability analysis [1], the nonlinear differential equations are solved by using step-by-step numerical integration techniques. Equations for generating units and other dynamic devices in the power systems can be expressed as follows:

$$\dot{\mathbf{x}}_{\mathbf{d}} = \mathbf{f}_{\mathbf{d}}(\mathbf{x}_{\mathbf{d}}, \mathbf{V}_{\mathbf{d}}) \tag{2.9}$$

$$\mathbf{I}_{\mathbf{d}} = \mathbf{g}_{\mathbf{d}}(\mathbf{x}_{\mathbf{d}}, \mathbf{V}_{\mathbf{d}}) \tag{2.10}$$

where

$\mathbf{x}_{\mathbf{d}}$ = state vector of individual device

$\mathbf{I}_{\mathbf{d}}$ = *R* and *I* components of current injection from the device into the network

$\mathbf{V}_{\mathbf{d}}$ = *R* and *I* components of bus voltage

The overall system equations, including the differential equations (2.9) for all the devices and combined algebraic equations for the devices and the network are expressed in the following general form comprising a set of first order differential equations

$$\dot{\mathbf{x}} = \mathbf{f}(\mathbf{x}, \mathbf{V}) \tag{2.11}$$

and a set of algebraic equations

$$\mathbf{I}(\mathbf{x}, \mathbf{V}) = \mathbf{Y}_{\mathbf{N}} \mathbf{V} \tag{2.12}$$

with a set of known initial conditions $(\mathbf{x}_{\mathbf{0}}, \mathbf{V}_{\mathbf{0}})$, where

$\mathbf{x}$ = state vector of the system

$\mathbf{V}$ = bus voltage vector

$\mathbf{I}$ = current injection vector

Depending on the modeling of the devices, and computational capabilities, several approaches are available to solve these equations. Numerical techniques most widely used are the Euler method, Modified Euler method and Runge-Kutta (R-K) methods [1]. These methods essentially utilize the Taylor series expansions to solve the equations.

2.2.4 DIRECT METHOD OF TRANSIENT STABILITY ANALYSIS – TRANSIENT ENERGY FUNCTION APPROACH

The direct methods determine the stability without explicitly solving the system differential equations. The transient energy function approach and its application to the power systems stability is explained in detail.

The transient energy approach can be described by considering a ball rolling on the inner surface of a bowl as shown in Figure 2.6 [1].

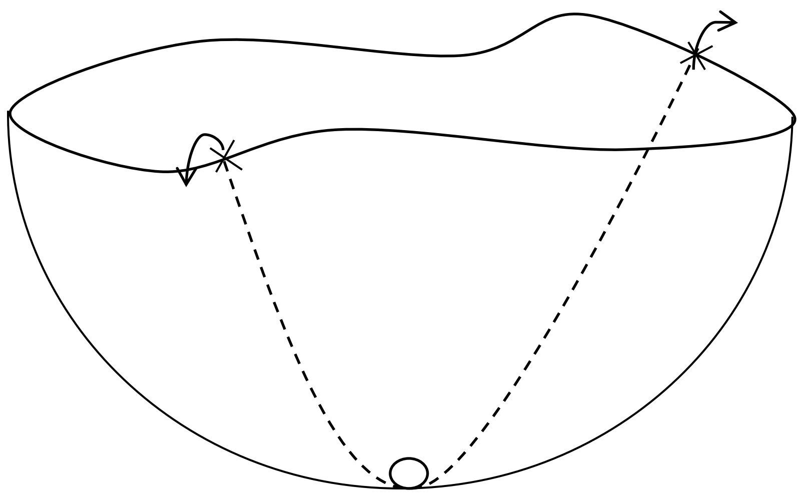

Figure 2.6 A ball rolling on the inner surface of a bowl

The area inside the bowl represents the stability region and the region outside is the region of instability. The rim has different heights at different points which represent different operating boundaries. Initially, the ball rests at the bottom of the bowl, this state is referred as stable equilibrium point (SEP). When the ball is injected by some kinetic energy, it moves in the direction determined by the applied energy. If the ball is able to convert all the kinetic energy into potential energy before crossing the boundary, then it rolls back to the SEP. If the kinetic energy applied is high enough to force the ball outside the rim, then the ball enters into the region of instability and it will never return to SEP. The surface inside the bowl represents the *potential energy surface* and the rim of the bowl represents the *potential energy boundary surface* (PEBS).

Application of this technique to power systems can be analyzed in a similar way. The system is initially at stable equilibrium point. If a fault occurs, the generators oscillate and the system gains kinetic and potential energy and moves away from the SEP. After fault clearing, the kinetic energy is converted into potential energy. To avoid instability, the system must be capable of absorbing the kinetic energy at a time when the forces are trying to bring the system back to equilibrium point. For a post disturbance condition, there is a maximum or critical amount of energy that the system can absorb. Assessment of transient stability requires functions that describe the transient energy responsible to separate one or more synchronous machines from the rest of the system and an estimate of *critical energy* required for the system to lose synchronism.

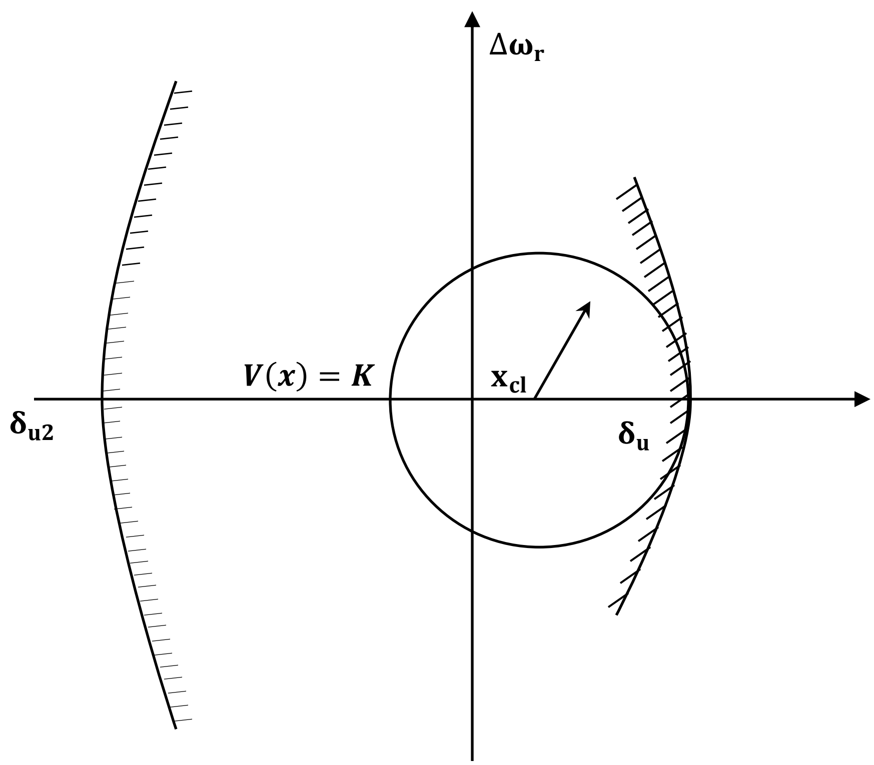

Figure 2.7 Region of stability and its local approximation

When a disturbance occurs, there is a stable equilibrium point for the post fault system. A region of attraction can be defined for this post fault SEP as shown in Figure 2.7 [1]. The post fault trajectory for which the state of system at fault clearing ($\mathbf{x_{cl}}$) lies inside this region of attraction will eventually converge to the SEP, and the system is said to be stable. On the other hand, if $\mathbf{x_{cl}}$ lies outside the region of attraction, the post fault system will not converge to the stable equilibrium point and the system is said to be unstable.

The direct method solves the stability problem by comparing $\boldsymbol{V}(\mathbf{x_{cl}})$ which is the value of energy function evaluated at $\mathbf{x_{cl}}$ to the critical energy V_{cr}. The system is stable if $\boldsymbol{V}(\mathbf{x_{cl}})$ is less than V_{cr} and the quantity $V_{cr} - \boldsymbol{V}(\mathbf{x_{cl}})$ is a good measure of system relative stability and is called *transient energy margin*.

As shown in Figure 2.7, if the rotor oscillates within the range δ_{u1} and δ_{u2} , the system will remain transiently stable and if the rotor swings beyond this limits, the system becomes unstable. These two points δ_{u1} and δ_{u2} form a boundary for stable oscillations and is called *potential energy boundary surface* (PEBS). The boundary of the stability region is approximated locally by a constant energy surface $\{\mathrm{x}|V(\mathrm{x}) = K\}$ as shown in Figure 2.7, where K represents the critical energy V_{cr} of the post fault system.

Application of the direct methods to power systems is limited to simple representation of generator and load models [1]. These methods are vulnerable to numerical problems while solving stressed systems. Heavy computational burden involved may increase the time taken to solve the problem, making it slower than time-domain simulations.

2.3 Voltage Stability

Voltage stability problems generally occur in heavily stressed systems. The underlying problem is the inherent weakness in the power system. The reason for this is that the system is not designed for every possible disturbance, because this is impossible and uneconomical. The main factors affecting the voltage stability are strength of transmission network, power transfer levels, generator reactive power/voltage control limits, load characteristics, characteristics of reactive power compensating devices, and voltage control devices such as under load tap changing transformers (ULTCs).

The voltage stability phenomenon can be examined by considering the relationships between the transmitted power (P_R), receiving end voltage (V_R), and the reactive power injection (Q_i). These characteristics are presented for the simple radial system shown in Figure 2.8.

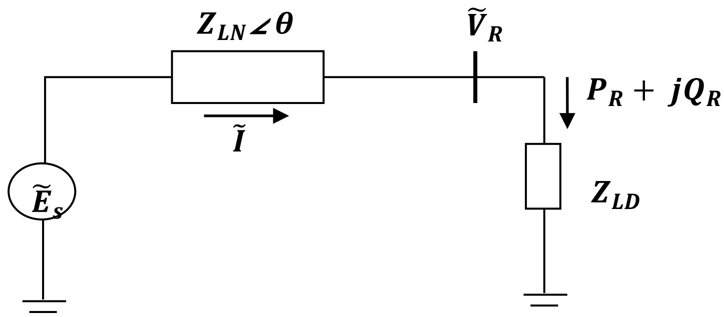

Figure 2.8 A simple radial system for illustration of voltage stability phenomenon

The current I and receiving end voltage V_R and power P_R are given by the following equations:

$$I = \frac{1}{\sqrt{F}} \frac{E_s}{Z_{LN}} \tag{2.13}$$

$$V_R = \frac{1}{\sqrt{F}} \frac{Z_{LD}}{Z_{LN}} E_s \tag{2.14}$$

$$P_R = \frac{Z_{LD}}{F} \left(\frac{E_s}{Z_{LN}}\right)^2 \cos\phi \tag{2.15}$$

Where

$$F = 1 + \left(\frac{Z_{LD}}{Z_{LN}}\right)^2 + 2\left(\frac{Z_{LD}}{Z_{LN}}\right)\cos(\theta - \phi)$$

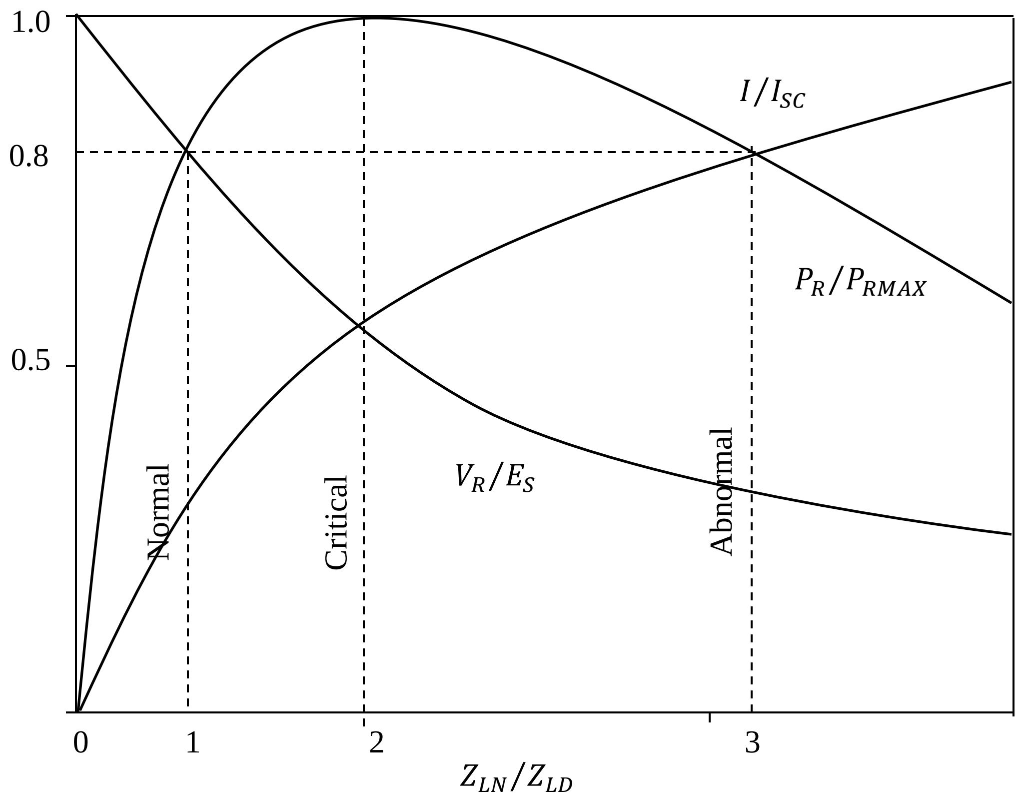

Figure 2.9 Receiving end voltage, current and power as a function of load demand

Figure 2.9 shows the plots of I, V_R and P_R as a function of load demand Z_{LN}/Z_{LD} for the case with $\tan\theta = 10.0$ and $\cos\phi = 0.95$. As load demand increases, P_R increases suddenly at first, slowly at the maximum value and then decreases. The values of V_R and I corresponding to maximum power are referred to as *critical values*. For a given value of P_R, there are two operating points corresponding to two different values of Z_{LD}. This is shown in Figure 2.9 for $P_R = 0.8$. The point to the left corresponds to the normal operation. For the point to the right, I is much larger and V_R is much smaller than the point to the left. This corresponds to the abnormal operation and is highly undesirable. For a load demand higher than the maximum power, control of power by varying load would be unstable. The increase in load admittance would decrease the power. The load characteristics and the action of voltage control devices have an adverse effect on the voltage and may cause it do decrease progressively. This phenomenon is called *voltage instability.*

2.4 VOLTAGE STABILITY ANALYSIS

The *V-P* and *Q-V* characteristics have been most widely used for the voltage stability analysis. Figure 2.10 shows the relation between receiving end voltage and power for load

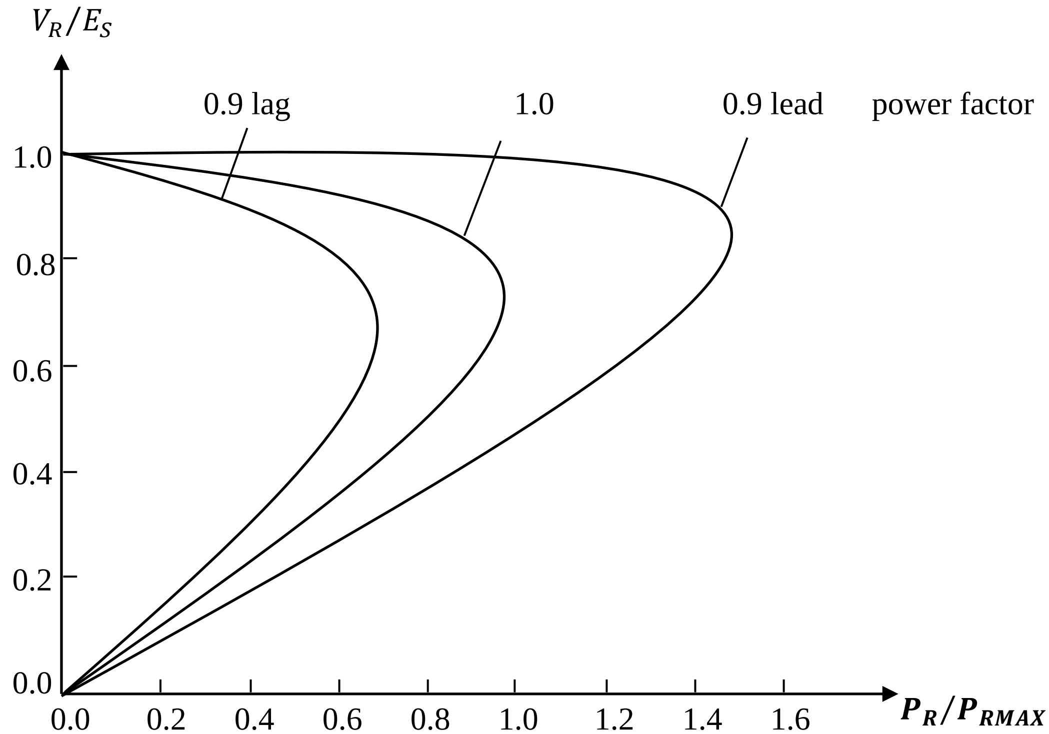

Figure 2.10 The V_R-P_R characteristics of the system of Figure 2.8

at different power factors These correspond to the simple radial system considered in Figure 2.8 [5]. These curves are produced by using a series of power flow solutions for different load levels. For each curve, the load in a certain area under consideration is uniformly scaled up while maintaining the power factor constant. At the "knee" of the *V-P* curve, the voltage drops rapidly with increase in load demand. Power – flow solution fails to converge, which is indicative of instability. Operating the system at stability limits is unsecure and a satisfactory operating condition is ensured by allowing sufficient "power margin".

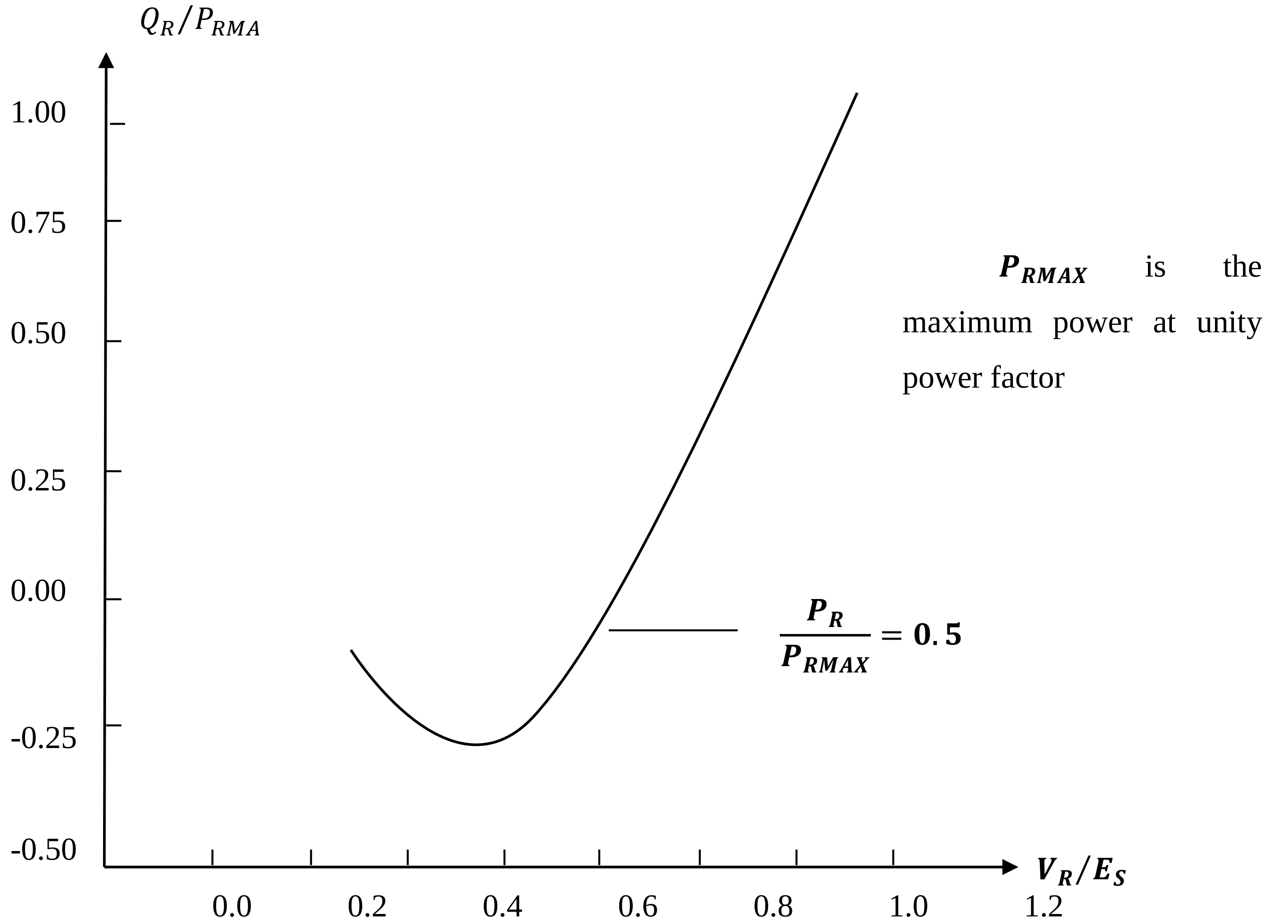

Figure 2.11 $V_{R-}Q_R$ characteristics of the system of Figure 2.8 with $\frac{P_R}{P_{RMAX}} = 0.5$

Voltage stability is affected considerably by the variations in Q (reactive power consumption) at the loads. A more useful characteristic for voltage stability analysis is the *Q-V* relationship, which shows the sensitivity of bus voltages with respect to reactive power injections and absorptions. The bottom of the *Q-V* curve, where the derivative dQ/dV is equal to zero, represents the voltage stability limit. Operation on the right side of *Q-V* curve is stable and on the left side is unstable.

2.4.1 Dynamic Analysis

As discussed previously (Section Transient Stability Analysis), dynamic analysis of power systems involve solution for first order differential equations, which can be expressed in the following general form:

$$\dot{\mathbf{x}} = \mathbf{f}(\mathbf{x}, \mathbf{V}) \tag{2.16}$$

and a set of algebraic equations

$$\mathbf{I}(\mathbf{x}, \mathbf{V}) = \mathbf{Y_N V} \tag{2.17}$$

with a set of known initial conditions $(\mathbf{x_0}, \mathbf{V_0})$, where

$\mathbf{x} =$ state vector of the system

$\mathbf{V} =$ bus voltage vector

$\mathbf{I} =$ current injection vector

$\mathbf{Y_N} =$ network node admittance matrix

The representation of transformer tap-changers and phase-shift angle controls are also included in the model, due to which the elements of $\mathbf{Y_N}$ change as a function of bus voltage and time. The current injection vector $\mathbf{I}$ is a function of the system states $\mathbf{x}$ and bus voltage vector $\mathbf{V}$, representing the boundary conditions at the terminals of the various devices. Equations (2.16) and (2.17) can be solved in time-domain using numerical techniques and network power flow analysis methods. The study period is typically on the order of several minutes.

2.4.2 STATIC ANALYSIS

The static approach captures snapshots of the system conditions at various time frames along the time domain trajectory. In this method, the overall system equations reduce to purely algebraic equations allowing the use of static analysis techniques. Practical applications are developed on the basis of *V-Q* sensitivity. The advantages of the modal analysis and sensitivity analysis are that they give voltage stability related information from a *system – wide* perspective and clearly identify areas that have potential problems.

2.4.3 V-Q SENSITIVITY ANALYSIS

The network constraints represented by Equation (2.17) can be expressed in the following linearized form:

$$\begin{bmatrix} \Delta\mathbf{P} \\ \Delta\mathbf{Q} \end{bmatrix} = \begin{bmatrix} \mathbf{J}_{\mathbf{P\theta}} & \mathbf{J}_{\mathbf{PV}} \\ \mathbf{J}_{\mathbf{Q\theta}} & \mathbf{J}_{\mathbf{QV}} \end{bmatrix} \begin{bmatrix} \Delta\boldsymbol{\theta} \\ \Delta\mathbf{V} \end{bmatrix} \tag{2.18}$$

where

$\Delta\boldsymbol{P} =$ incremental change in bus real power

$\Delta\boldsymbol{Q} =$ incremental change in bus reactive power injection

$\Delta\boldsymbol{\theta} =$ incremental change in bus voltage angle

$\Delta\boldsymbol{V} =$ incremental change in bus voltage magnitude

$\mathbf{J}_{\mathbf{xy}} =$ $\mathbf{dx/dy}$

The elements of the Jacobian matrix give the sensitivity between power flow and bus voltage changes. System voltage stability is affected by both *P* and *Q*. In this analysis, at each operating point, *P* is kept constant and voltage stability is analyzed by considering the incremental relationship between *Q* and *V*. Based on these considerations, in Equation (2.18), let $\Delta\mathbf{P} = \mathbf{0}$. Then

$$\Delta\mathbf{Q} = \mathbf{J}_{\mathbf{R}}\Delta\mathbf{V} \tag{2.19}$$

where

$$\mathbf{J}_{\mathbf{R}} = \left[\mathbf{J}_{\mathbf{QV}} - \mathbf{J}_{\mathbf{Q\theta}}\mathbf{J}_{\mathbf{P\theta}}^{-1}\mathbf{J}_{\mathbf{PV}}\right] \tag{2.20}$$

and $\mathbf{J}_{\mathbf{R}}$ is the reduced Jacobian matrix of the system. From Equation (2.20), we can write

$$\Delta\mathbf{V} = \mathbf{J}_{\mathbf{R}}^{-1}\Delta\mathbf{Q} \tag{2.21}$$

The matrix $\mathbf{J}_{\mathbf{R}}^{-1}$ is the reduced *V-Q* Jacobian. Its i^{th} diagonal element is the *V-Q* sensitivity at bus i. A positive *V-Q* sensitivity is indicative of stable operation; the smaller the stability, more stable the system. As stability decreases, the magnitude of the sensitivity increases. A negative sensitivity is indicative of unstable operation. A small negative sensitivity represents a very unstable operation.

2.4.4 Q-V MODAL ANALYSIS

Voltage stability characteristics of the system can be identified by computing eigenvalues and eigenvectors of the reduced Jacobian matrix $\mathbf{J_R}$ defined by Equation (2.20). This matrix can be decomposed into left eigenvector, right eigenvector, and eigenvalue matrices as shown

$$\mathbf{J_R} = \boldsymbol{\xi}\,\boldsymbol{\Lambda}\,\boldsymbol{\eta} \tag{2.22}$$

where

$\boldsymbol{\xi} =$ Right eigenvector matrix of $\mathbf{J_R}$

$\boldsymbol{\Lambda} =$ Left eigenvector matrix of $\mathbf{J_R}$

$\boldsymbol{\eta} =$ Diagonal eigenvalue matrix of $\mathbf{J_R}$

Rearranging Equation (2.22) and substituting it in Equation (2.21) gives

$$\Delta\mathbf{V} = \sum_{i} \frac{\boldsymbol{\xi}_i \boldsymbol{\eta}_i}{\lambda_i}\,\Delta\mathbf{Q} \tag{2.23}$$

Where $\boldsymbol{\xi}_i$ is the i^{th} column right eigenvector and $\boldsymbol{\eta}_i$ the i^{th} row left eigenvector of $\mathbf{J_R}$. Each eigenvalue $\boldsymbol{\lambda}_i$ and the corresponding right and left eigenvectors $\boldsymbol{\xi}_i$ and $\boldsymbol{\eta}_i$ define the i^{th} mode of the *Q-V* response. The modal analysis is performed using the Equation (2.24).

$$\mathbf{v} = \boldsymbol{\Lambda}^{-1}\mathbf{q} \tag{2.24}$$

where

$\mathbf{v} = \boldsymbol{\eta}\,\Delta\mathbf{V}$ is the vector of modal voltage variations

$\mathbf{q} = \boldsymbol{\eta}\,\Delta\mathbf{Q}$ is the vector of modal reactive power variations

In Equation (2.24), $\mathbf{\Lambda}^{-1}$ is a diagonal matrix and this equation represents uncoupled first order equations. For the i^{th} mode we have

$$\mathbf{v_i} = \frac{1}{\lambda_i}\mathbf{q_i} \tag{2.25}$$

The stability criterion is formulated as follows. If $\lambda_i > 0$, then the system is voltage stable. If $\lambda_i < 0$, then the system is voltage unstable. The magnitude of λ_i determines the degree of stability of the i^{th} modal voltage. The smaller the magnitude of positive λ_i, the closer the i^{th} modal voltage to being unstable. When $\lambda_i = 0$, i^{th} modal voltage collapses because any change in that modal reactive power causes infinite change in the corresponding modal voltage.

2.5 PATTERN RECOGNITION

As discussed previously in section 1.5, "Pattern recognition is the study of how machines can observe the environment, learn to distinguish patterns of interest from their background, and make sound and reasonable decisions about the categories of the pattern" [22]. The two methods the author has used are Regularized Least Squares Classification (RLSC) and Classification and Regression Trees (CART). The detailed explanation of these methods is presented.

2.5.1 REGULARIZED LEAST SQUARES CLASSIFICATION (RLSC)

The basic idea of this algorithm is to fit the "training" set of data $S_m = (x_i, y_i)_{i=1}^m$ with a function $f: X \to Y -$ with X a closed subset of $\mathbb{R}^n$ and $Y \subset \mathbb{R} -$ that generalizes, or is predictive. This algorithm can be derived from Tikhonov regularization [36] .

We consider the data $S = (x_i, y_i)_{i=1}^m$ where y_i takes values $\{-1, +1\}$. The goal is to come up with a function $f(x)$ while minimizing the probability of error described by Equation (2.26).

$$P\,r\left(sgn\big(f(x)\big)\right) \neq y \tag{2.26}$$

This can be found by solving the problem – called Empirical Risk Management (ERM) – of finding the function in $\mathcal{H}$ which minimizes

$$\frac{1}{m}\sum_{i=1}^{m}(f(x_i)-y_i)^2 \tag{2.27}$$

which is in general *ill-posed*, depending on the choice of the hypothesis space $\mathcal{H}$. Following Tikhonov we minimize, instead, over the hypothesis space $\mathcal{H}_K$, for a fixed positive parameter γ, the regularized functional M_2:

$$\mathrm{M}_2 = \frac{1}{m}\sum_{i=1}^{m}(f(x_i)-y_i)^2 + \gamma\|f\|_k^2 \tag{2.28}$$

where $\|f\|_k^2$ is the norm in $\mathcal{H}_K$ – the Reproducing Kernel Hilbert Space (RKHS), defined by the kernel K.

The solution for Tikhonov regularization problem can be solved by Representer Theorem [37] and is:

$$f(x) = \sum_{i=1}^{n} c_i k(x, x_i) \tag{2.29}$$

The solution is obtained as follows. First, the kernel matrix K is constructed from the training set S.

$$K = \left(k_{ij}\right)_{1\le i,j\le n} \qquad\qquad k_{ij} = k\left(x_i, x_j\right)$$

Next step is to compute the vector coefficients $c = (c_1, c_2, \dots, c_n)^T$ by solving the system of linear equations

$$(K + n\lambda I)c = y \tag{2.30}$$

$$c = (K + n\lambda I)^{-1}\, y \tag{2.31}$$

where $y = (y_1, y_2, \dots, y_n)^T$, I is the identity matrix of dimension n and finally, the classifier is

$$f(x) = \sum_{i=1}^{n} c_i k(x, x_i) \tag{2.32}$$

The sign of this function $f(x)$ decides the class $(+1\ or -1)$ for the instance x and its magnitude is the confidence in this prediction.

2.5.2 Data Mining – Classification and Regression Trees (CART)

Data mining is the process of extracting knowledge from data. The goal is to extract rules or knowledge from regularity patterns exhibited by the data. Decision Trees (DTs) is a method used for Data Mining. CART (Classification and Decision Trees) is the methodology used to build the DTs. The main focus, due to the nature of our problem, is on classification trees. Salford System's data mining software CART® is used for the analysis.

A Decision Tree is a form of inductive learning. For a given data set, the objective is to build a model that captures the mechanism that gave rise to the data. The process of constructing the model is a "Supervised learning" problem since the training is supervised by an outcome variable called the target [38]. Figure 2.12 shows a schematic view of a decision tree. Decision Trees are grown through a systematic method known as recursive binary partitioning; where successive questions with yes/no answers are asked in order to partition the sample space.

The process begins with a "root" node that encloses the learning sample L. At each node t the sample is split into two subsets t_L and t_R, the left and right child respectively. The splitting process is iterated until the terminal node is reached, i.e. a node where no further split is possible. A classification decision is made at such terminal nodes.

The learning sample L is composed by a set of measurements vectors $X = \{x_1, x_2, \dots, x_m\}$. Each column of a measurement vector x_i is known as an attribute. An attribute can be either numerical or categorical. Categorical attributes take a finite set of values and do not have an intrinsic order; for example: temperature = {cold, hot}. On the other hand, numerical attributes take value in a real line and therefore have a natural order.

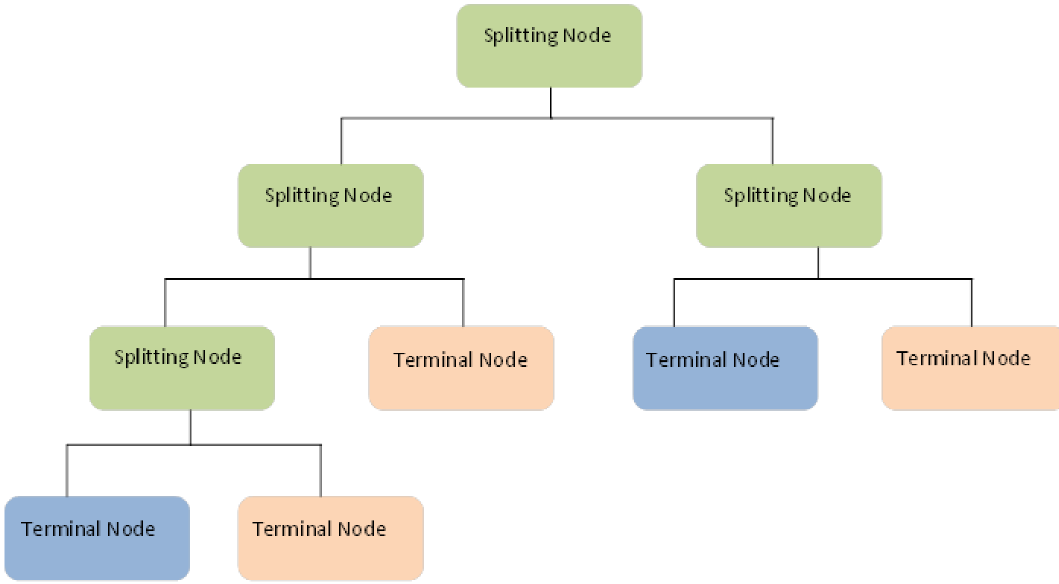

Figure 2.12 Classification Trees - After a successive sample partitions a classification decision is made at the terminal nodes

Being a supervised learning method, the class of each vector must be known prior to data mining process. Therefore, each measurement vector x_i must be classified into a set of mutually exclusive classes $C = \{C_1, C_2, \dots, C_J\}$.

Table 2-1 Learning sample matrix with n attributes and m measurement vectors

	Target	Attr 1	Attr 2	Attr 3	. . .	Attr n
$\boldsymbol{x_1}$	C_j	numerical	categorical	. . .	. . .	. . .
$\boldsymbol{x_2}$	. . .	. . .	. . .	. . .	. . .	. . .
. . .	. . .	. . .	. . .	. . .	. . .	. . .
$\boldsymbol{x_m}$	. . .	. . .	. . .	. . .	. . .	. . .

In general, the learning sample L is a matrix with m rows (the number of measurement vectors) and $n + 1$ columns (the number of attributes on each measurement vector plus the target).

2.5.2.1 Growing Decision Trees

The process begins at the root node which encloses the learning sample L . The idea is to partition the space into disjoint subsets so as to increase the "purity". Purity can be understood as a measurement of class homogeneity. Homogeneous nodes that include only one class C_j achieve maximum purity, whereas heterogeneous nodes with an equal proportion of classes $C_0, \dots, C_j$ have minimum purity.

A split is said to be optimal when it maximizes the purity of the descendent nodes. For convenience, optimality can be expressed in terms of node impurity rather than purity. In this case, optimal split should minimize the impurity. Gini index, Entropy Impurity, Towing are some of the impurity functions generally used [38]. However, empirical results suggest that the choice of a particular impurity function has little effect in the selection of a final tree [39]. The most commonly used index is called "Gini Impurity index", and is defined as follows:

$$i(t) = 1 - \sum_{j}^{J} p^2\left(C_j|t\right) \tag{2.33}$$

where $p\left(C_j\middle|t\right)$ is an estimator of the probability that a case belongs to class C_j given that it falls into t.

Then, the goodness-of-split criterion of a split s at node t is defined to be the decrease in impurity achieved by split s,

$$\Delta i(s,t) = i(t) - [\, p_L. i(t_L) + p_R. i(t_R)] \tag{2.34}$$

where $i(t)$ is impurity measurement at node t computed using equation (2.33), p_L and p_R are the proportion of cases that fall into the left and right child respectively, and $i(t_L)$ and $i(t_R)$ are the left and right child impurity measurements.

The optimal split $\boldsymbol{s_{optimal}}$ is defined to be the split that maximizes the decrease in impurity in equation (2.34). To find such a split, CART performs an exhaustive search over all attributes and all possible splitting values.

Let us consider the set of attributes $A = \{a_1, a_2, \ldots, a_n\}$. Each attribute $a \in A$ is iteratively selected one at a time. If the selected attribute is numerical, then there are an infinite number of possible splitting values. It is customary, though completely arbitrary, to select the midpoint between two adjacent values splitting rule. If the selected attribute is categorical, then there are a finite number of splitting thresholds and they are set of unique categories in A.

Let us define $S_a = \{s_1, s_2, \ldots\}$ to be the set of potential splitting values of attribute a. The optimal split s_a of attribute a is the one that maximizes the decrease in impurity expressed by equation (2.34). Finally, $\boldsymbol{s_{optimal}}$ at node t is the split that maximizes the decrease in impurity $\Delta i(s,t)$ over all the attributes $a \in A$ and splitting values $s \in S_a$.

Following this systematic procedure, the tree is grown by recursively finding optimal splits and partitioning each node into two children. CART's algorithm initially grows a tree as large as possible. A node is considered to be terminal if it has achieved zero impurity or if the total number of measurement vectors x_i at node t is less than some predetermined value n_{min}.

Finally, a classification decision is made at the terminal nodes. Class C_j is assigned to terminal node if $p(C_j|t)$ is the largest,

$$p(C_j|t) = \max_i(\, p(C_i|t)\,) \tag{2.35}$$

In this thesis, the classification of voltage stable and unstable cases simulated using PSSE is done. This can be considered as a binary classification problem. The CART trees and final results are presented in chapter 5.

Chapter 3

3 POWER SYSTEM MODELS FOR SIMULATION

In this chapter, the software package used for the dynamic simulation of the power system, PSS®E is explained. Models of the power systems equipment used in this thesis are presented.

3.1 INTRODUCTION

Power System Simulator for Engineering (PSS®E) is composed of a comprehensive set of programs for studies of power system transmission network and generation performance in both steady-state and dynamic conditions. Currently two primary simulations are used, one for steady-state analysis and one for dynamic simulations. PSS/E can be utilized to facilitate calculations for a variety of analyses, including:

• Power flow and related network functions

• Optimal power flow

• Balanced and unbalanced faults

• Network equivalent construction

• Dynamic simulation

In addition, to the steady-state and dynamic analyses, PSS®E also provides the user with a wide range of auxiliary programs for installation, data input, output, manipulation and preparation. The main focus of this chapter is on the dynamic simulation of the power system.

3.2 POWER SYSTEM SIMULATOR FOR ENGINEERING (PSSE)

The dynamic simulation model library of PSS®E represents a wide, and constantly growing, variety of electromechanical equipment. These models are called by subroutines while performing the dynamics simulation. The users can also create their own models if needed. The models of electrical equipment used in this thesis are as follows.

3.2.1 GENERATOR MODEL

The generator model presents the electric transmission network with a positive sequence source voltage where instantaneous amplitude and phase are known and where current is to be determined. Generally, a generator is thought of as a voltage source behind the step up transformer and dynamic impedance but in PSS®E, it is represented by a Norton equivalent in which a voltage source is replaced by an equivalent current source, ISORCE.

Rotor flux linkage transients and magnetic saturation are the principal factors affecting the dynamic behavior of synchronous machines. The magnitude and phase currents at any instant are determined at any instant as a function of the instantaneous values of generator state variables (i.e., rotor circuit flux linkages, shaft speed and rotor angle).

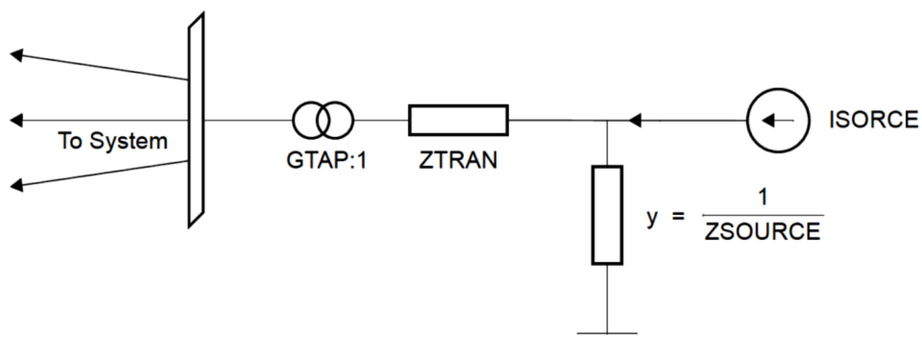

Figure 3.1 Generator model equivalent current source and Norton Equivalent Circuit [39]

The synchronous generator model used in this thesis is GENROU and its modeling is shown in Figure 3.2. The reactances and time constants used for modeling are presented in Table 3-1.

Table 3-1 Reactances and Time Constants used for modeling

Reactances and Time Constants	Description
$\mathbf{X_d}$	Synchronous Reactance
$\mathbf{X_q}$	
$\mathbf{X'_d}$	Transient Reactance
$\mathbf{X'_q}$	
$\mathbf{X''_d}$	Sub-Transient Reactance
$\mathbf{X''_q}$	
$\mathbf{X_l}$	Armature Leakage Reactance
$\mathbf{T'_{do}}$	Transient OC Time Constant
$\mathbf{T'_{qo}}$	
$\mathbf{T''_{do}}$	Sub-Transient OC Time Constant
$\mathbf{T''_{qo}}$	
$\boldsymbol{S(1.0), S(1.2)}$	Saturation Factors

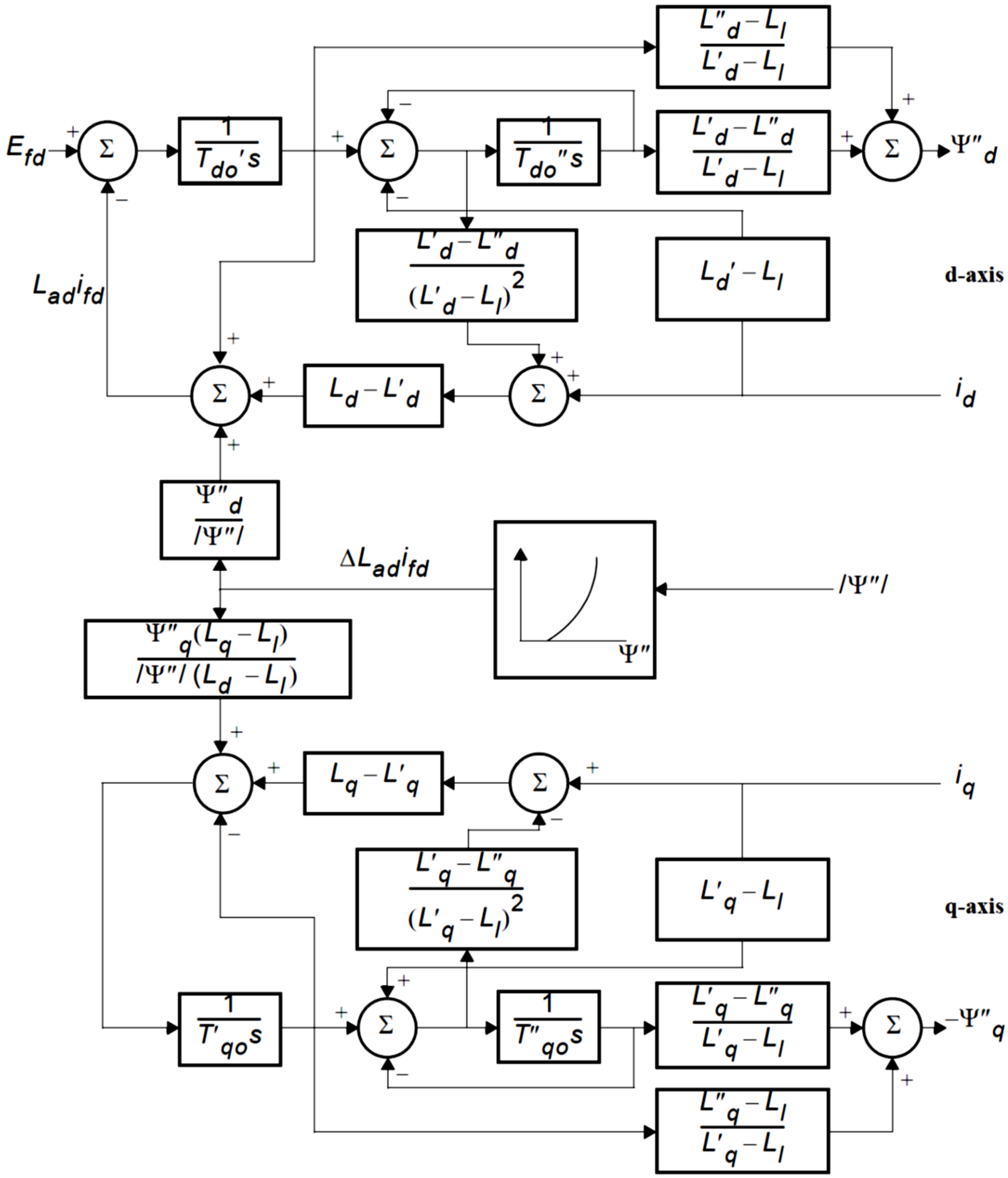

Figure 3.2 Electromagnetic Model of Round Rotor Generator (GENROU) [39]

3.2.2 EXCITATION SYSTEM MODEL

The basic approach to the excitation of large generators is shown in Figure 3.3. The excitation system consists of a high power source of direct current, an intermediate power level controlling circuit, and an instrument level voltage regulator. The voltage regulator determines the manipulation of the exciter. The proper representation of the excitation systems requires careful considerations of both the gains and time constants assigned to the voltage regulators and of the excitation power components.

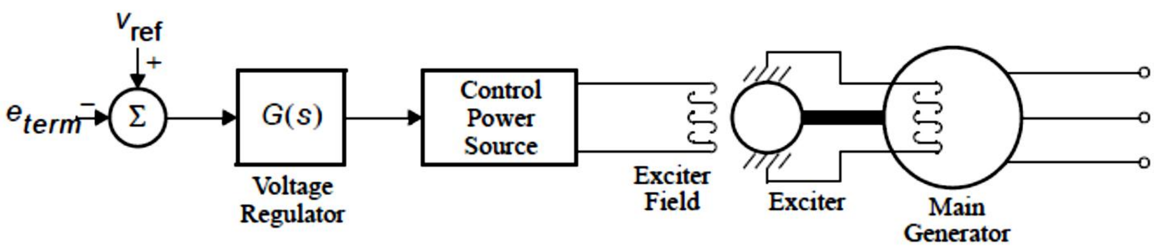

Figure 3.3 Rotating DC Exciter [39]

The excitation system model used in this thesis is ESDC1A. The type DC1A exciter model represents field-controlled dc commutator exciters, with continuously acting voltage regulators. The exciter may be separately excited or self-excited, the latter type being more common. The complete model of ESDC1A excitation system is shown in Figure 3.4.

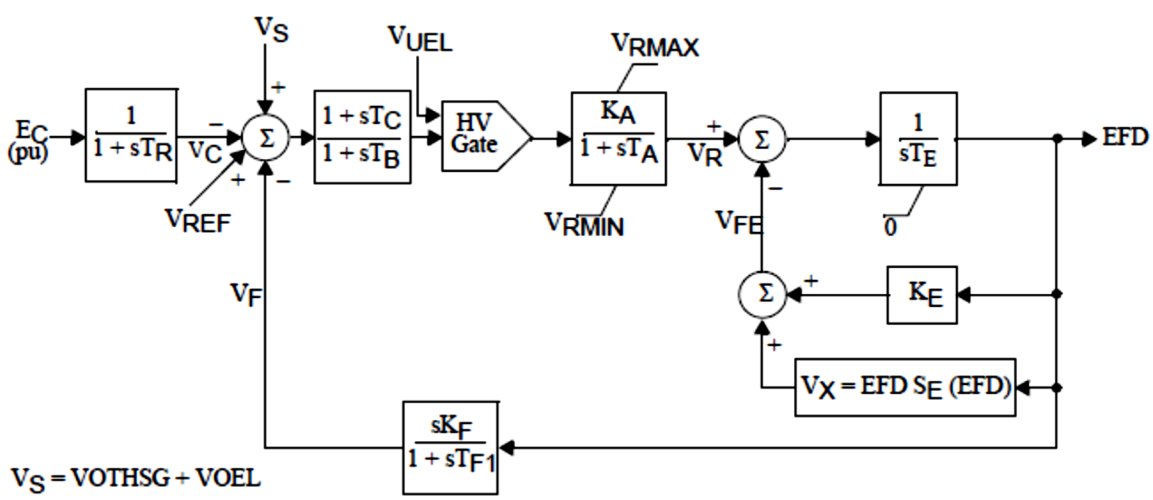

Figure 3.4 ESDC1A excitation system model [39]

3.2.3 MAXIMUM EXCITATION LIMITER MODEL

The limiters do not come into play in normal operating conditions. These circuits are important for long-term stability and voltage stability studies. The limiter is set to operate when the field current exceeds a certain pre-defined value Maximum excitation limiters are designed to protect the generator field of an ac machine with automatic excitation control from overheating due to prolonged over-excitation, which can be caused either by failure of a component of the voltage regulator or an abnormal system condition.

The PSSE model used in this thesis is MAXEX1. It acts through the regulator to correct an overexcitation problem. This model assumes an inverse time characteristic as shown in Figure 3.5; i.e., operating time is a function of the magnitude of the overvoltage.

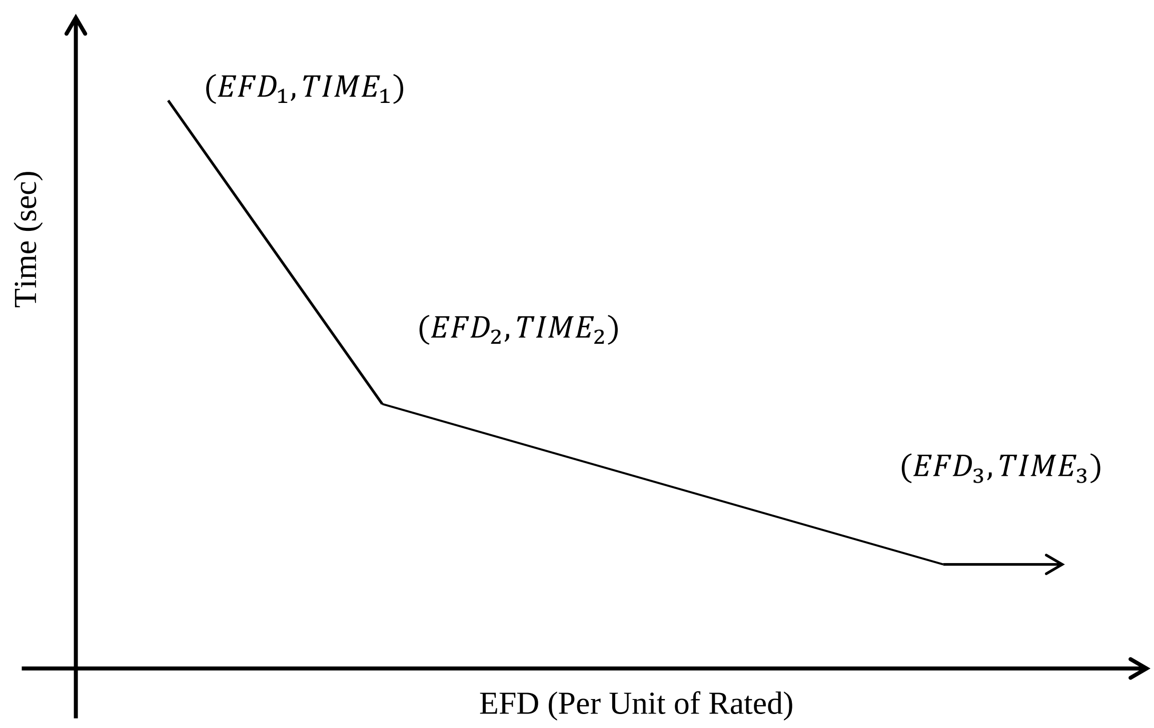

Figure 3.5 Inverse Time characteristics of MAXEX1

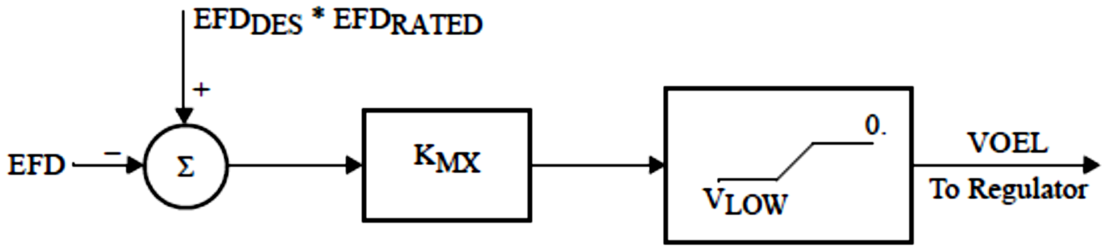

Figure 3.6 Block Diagram of MAXEX1 [39]

The operation of MAXEX1 is as follows:

1. Below EFD_1, the device is inactive
2. Above EFD_3, the time to operate is constant and equal to $TIME_3$.
3. If EFD goes below EFD_1 at any time before the device has timed out, the timer resets.

The values of $EFD_1, EFD_2, and\ EFD_3$ and $TIME_1, TIME_2\ and\ TIME_3$ are tuned to operate the limiters as required by the exciter model.

3.2.4 Turbine Governor System Model

The prime mover governing system provides a means of controlling power and frequency, a function commonly referred to as automatic generation control (AGC). The turbine-governor models are designed to give representations of the effects of power plants on power system stability. The model used is IEEG3, which is a hydro governor model. The block diagram and the corresponding parameters are shown in Figure 3.7.

.

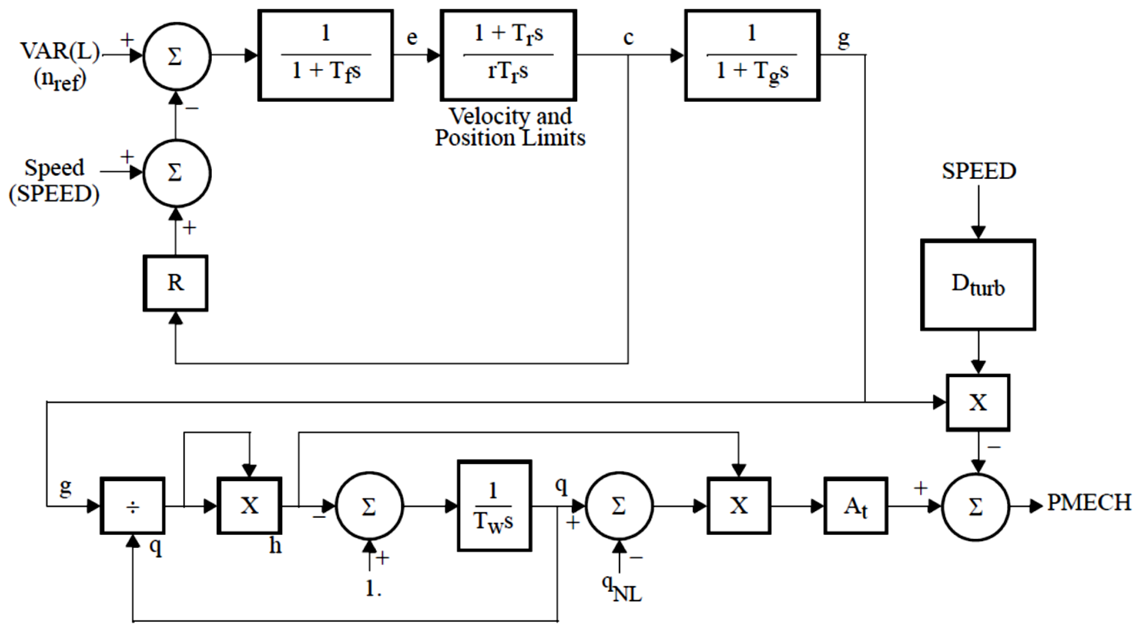

R	= Permanent droop	f	= Per unit flow
r	= Temporary droop	h	= Per unit Head
$\mathbf{T_r}$	= Governor time constant	$\mathbf{q_{NL}}$	= No power flow
$\mathbf{t_f}$	= Filter time constant	$\mathbf{A_t}$	= Turbine gain
$\mathbf{T_g}$	= Servo time constant	$\mathbf{D_{turb}}$	= Turbine damping
g	= Per unit gate opening		

Figure 3.7 IEEG3 hydro governor model [39]

3.2.5 Power System Stabilizer Model

The power system stabilizer (PSS) uses auxiliary stabilizing signals to control the excitation system so as to improve power system dynamic performance. Commonly used input signals to the power system stabilizer are shaft speed, terminal frequency and power. Power system dynamic performance is improved by the damping of system oscillations. The basic function of PSS is to add damping to the generator rotor oscillations by controlling its excitation using the auxiliary stabilizing signals. The model used in this thesis is PSS2A. The details of the model are shown in Figure 3.8.

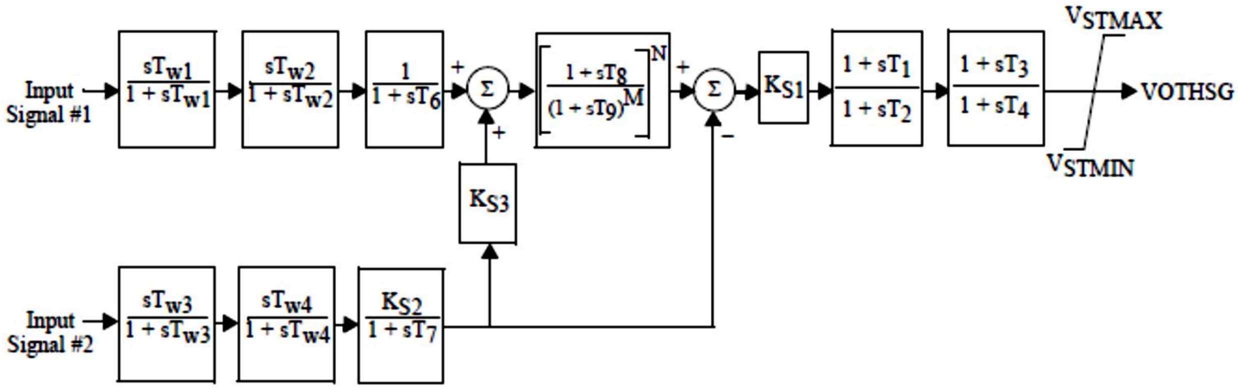

Figure 3.8 PSS2A Stabilizer Model [39]

In addition to the models described, on load tap changing transformers (OLTC1) are also used. All the dynamics models used are pre-defined in PSSE model library. The IEEE 39 bus system used and the values of the parameters for all the models described above are presented in Chapter 4.

Chapter 4

4 TEST SYSTEM

4.1 IEEE 39 BUS SYSTEM

The IEEE 39 bus system is the test bench study system used in this thesis. This is the reduced system for New England system. The objective of this reduced system is to retain an accurate small system representing the New England system. The system consists of 39 buses out of which 19 are load buses. There are 10 generators in the system. Bus 31 which

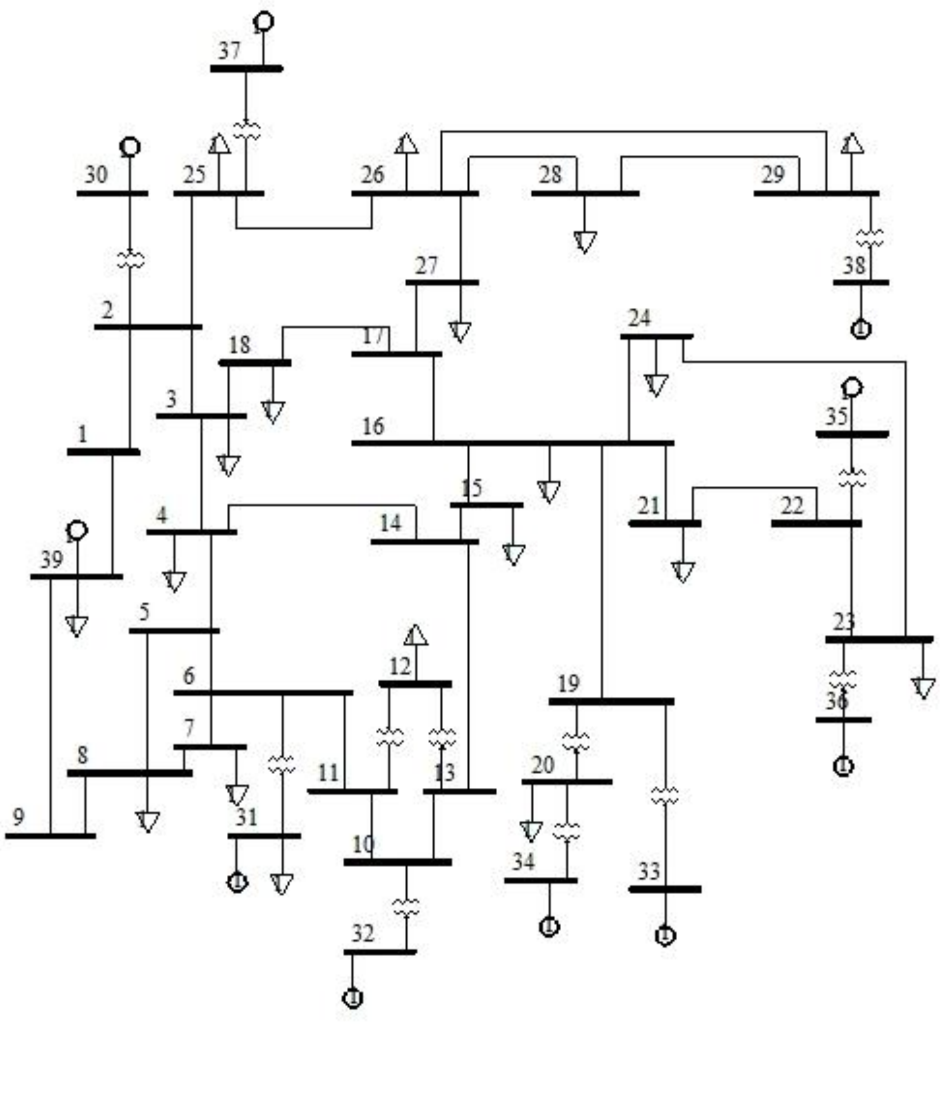

Figure 4.1 One line diagram of IEEE 39 bus system

has generator 3 is defined to be slack bus. The total load and generation in the system is 6150.1 MW and 6192.84 MW respectively. The load model is considered to be constant current (I) and constant admittance (Y) load. One line diagram of the system is shown in Figure 4.1. The power flow data and dynamics data of the models used are presented in the following sections.

4.2 BUS DATA

The test system consists of 39 buses. The voltage and angle values initially set are shown in Table 4-1. The buses 30 to 39 are PV buses, as they have generating plants, except bus 31 which is considered to be slack bus. It accommodates for the excess generation required. All the remaining buses are PQ buses. The voltages are in PU of 100 MVA base and corresponding bus voltage base.

Table 4-1 IEEE 39 Bus, bus data

Bus #	Bus Name	Base kV	Code	Voltage (PU)	Angle (Deg)
1	BUS_1	345	1	1.0445	-8.54
2	BUS_2	345	1	1.0412	-5.82
3	BUS_3	345	1	1.025	-8.68
4	BUS_4	345	1	1.0009	-9.68
5	BUS_5	345	1	1.0032	-8.67
6	BUS_6	345	1	1.0057	-8.01
7	BUS_7	345	1	0.9951	-10.19
8	BUS_8	345	1	0.9942	-10.69
9	BUS_9	345	1	1.0275	-10.41
10	BUS_10	345	1	1.0153	-5.48
11	BUS_11	345	1	1.0108	-6.34
12	BUS_12	345	1	0.9981	-6.31
13	BUS_13	345	1	1.0122	-6.16
14	BUS_14	345	1	1.0092	-7.72
15	BUS_15	345	1	1.0128	-7.79
16	BUS_16	345	1	1.0292	-6.23
17	BUS_17	345	1	1.0296	-7.34
18	BUS_18	345	1	1.0265	-8.28
19	BUS_19	345	1	1.0489	-1.06
20	BUS_20	345	1	0.9907	-2.05
21	BUS_21	345	1	1.0298	-3.82
22	BUS_22	345	1	1.0485	0.64
23	BUS_23	345	1	1.0436	0.44
24	BUS_24	345	1	1.035	-6.11

Continued…

Table 4-1 Continued…

25	BUS_25	345	1	1.0443	-4.18
26	BUS_26	345	1	1.0454	-5.47
27	BUS_27	345	1	1.0323	-7.49
28	BUS_28	345	1	1.0467	-1.93
29	BUS_29	345	1	1.0476	0.84
30	GEN_10	22	2	1.0475	-3.39
31	GEN_2	22	3	0.982	0
32	GEN_3	22	2	0.9831	2.51
33	GEN_4	22	2	0.9972	4.16
34	GEN_5	22	2	1.0123	3.14
35	GEN_6	22	2	1.0493	5.59
36	GEN_7	22	2	1.0635	8.3
37	GEN_8	22	2	1.0278	2.51
38	GEN_9	22	2	1.0265	7.91
39	GEN_1	345	2	1.03	-10.15

4.3 GENERATION DATA

As previously mentioned, there are 10 generating units the test system. The data corresponding to these generators are given in Table 4-2. The machine bases corresponding to the generators are given. The real and reactive powers generated for the base loading are shown. VSched is the scheduled voltage to be maintained at the terminals of the generators. The corresponding dynamics data is given in Table 4-3.

Table 4-2 IEEE 39 Bus, Generation data

Bus #	Code	Mbase (MVA)	PGen (MW)	QGen (MVar)	QMax (MVar)	QMin (MVar)	VSched (PU)
30	2	1290.00	250	187.5	200	-500	1.0475
31	3	574.00	524.2	203.7	350	-500	0.982
32	2	753.00	650	210.5	250	-500	0.9831
33	2	917.00	632	116.1	150	-500	0.9972
34	2	303.00	508	168.6	200	-300	1.0123
35	2	800.00	650	216.8	250	-500	1.0493
36	2	816.00	560	105.8	150	-500	1.0635
37	2	702.00	540	-84.4	50	-500	1.0278
38	2	702.00	830	38.1	50	-500	1.0265
39	2	6667.00	1000	103.4	200	-1000	1.03

Table 4-3 Generator Dynamics data

Model Name	T'do	T"do	T'qo	T"qo	H	Xd	Xq	X'd	X'q	X"d = X"q	Xl
GENROU	10.2	0.03	0.2	0.04	3.255	1.29	0.89	0.4	0.103	0.082	0.013
GENROU	6.56	0.03	1.5	0.04	5.28	1.693	1.618	0.4	0.967	0.2	0.035
GENROU	5.7	0.03	1.5	0.04	4.75	1.879	1.785	0.4	0.66	0.2	0.03
GENROU	5.69	0.03	1.5	0.04	3.117	2.403	2.367	0.4	1.523	0.2	0.03
GENROU	5.4	0.03	0.44	0.04	8.58	2.03	1.879	0.4	0.503	0.2	0.054
GENROU	7.3	0.03	0.4	0.04	4.35	2.032	1.928	0.4	0.651	0.2	0.022
GENROU	5.66	0.03	1.5	0.04	3.23	2.408	2.384	0.4	1.518	0.2	0.032
GENROU	6.7	0.03	0.41	0.04	3.46	2.035	1.965	0.4	0.639	0.2	0.028
GENROU	4.79	0.03	1.96	0.04	4.92	1.478	1.439	0.4	0.411	0.2	0.03
GENROU	7	0.03	0.7	0.04	7.5	1.333	1.267	0.4	0.533	0.2	0.003

4.4 LOAD DATA

There are 19 loads in the test system. The values are shown in Table 4-4. The values are given in MW for real loads and Mvar for reactive loads. These loads are converted into constant current (real loads) and constant impedance (reactive power) for dynamics simulations.

Table 4-4 IEEE 39 Bus, Load data

Bus Number	Pload (MW)	Qload (Mvar)
3	322	2.4
4	500	184
7	233.8	84
8	522	176
12	8.5	88
15	320	153
16	329	32.3
18	158	30
20	628	103
21	274	115
23	247.5	84.6

Continued…

Table 4-4 Continued…

24	308.6	-92
25	224	47.2
26	139	17
27	281	75.5
28	206	27.6
29	283.5	26.9
31	9.2	4.6
39	1104	250

4.5 BRANCH AND TRANSFORMER DATA

The transmission line data is given in Table 4-5. The values are in PU of 100 MVA and 345 KV base. The line model used is π equivalent circuit [1]. Determining the correct data for transformers is an important task in modeling a power system in PSS®E. The transformer data is given in Table 4-6. There are 12 transformers in the test system; out of 9 are voltage control transformers or On Load Tap Changing transformers (OLTC). The resistances and reactances are in PU of system MVA base and primary bus voltage base. There are 8 tap positions for each transformer, and the voltage is controlled on the primary side of the transformer. Vmax and Vmin are the voltage limits beyond which the tap changer is initiated. Rmax and Rmin determine the voltage range of the taps and are in PU of primary bus voltage base.

Table 4-5 IEEE 39 Bus, Branch data

From Bus #	To Bus #	Id	Line R (PU)	Line X (PU)	Charging (PU)
1	2	1	0.0035	0.0411	0.6987
1	39	1	0.001	0.025	0.75
2	3	1	0.0013	0.0151	0.2572
2	25	1	0.007	0.0086	0.146
3	4	1	0.0013	0.0213	0.2214
3	18	1	0.0011	0.0133	0.2138
4	5	1	0.0008	0.0129	0.1382
4	14	1	0.0008	0.0129	0.1382
5	6	1	0.0002	0.0026	0.0434
5	8	1	0.0008	0.0112	0.1476
6	7	1	0.0006	0.0092	0.113
6	11	1	0.0007	0.0082	0.1389
7	8	1	0.0004	0.0046	0.078
8	9	1	0.0023	0.0363	0.3804

Continued…

Table 4-5 Continued…

9	39	1	0.001	0.025	1.2
10	11	1	0.0004	0.0043	0.0729
10	13	1	0.0004	0.0043	0.0729
13	14	1	0.0009	0.0101	0.1723
14	15	1	0.0018	0.0217	0.366
15	16	1	0.0009	0.0094	0.171
16	17	1	0.0007	0.0089	0.1342
16	19	1	0.0016	0.0195	0.304
16	21	1	0.0008	0.0135	0.2548
16	24	1	0.0003	0.0059	0.068
17	18	1	0.0007	0.0082	0.1319
17	27	1	0.0013	0.0173	0.3216
21	22	1	0.0008	0.014	0.2565
22	23	1	0.0006	0.0096	0.1846
23	24	1	0.0022	0.035	0.361
25	26	1	0.0032	0.0323	0.513
26	27	1	0.0014	0.0147	0.2396
26	28	1	0.0043	0.0474	0.7802
26	29	1	0.0057	0.0625	1.029
28	29	1	0.0014	0.0151	0.249

Table 4-6 IEEE 39 Bus, Transformer data

From Bus #	To Bus #	Tap Positions	Specified R (PU)	Specified X (PU)	Wnd1 Ratio	Rmax (ratio)	Rmin (ratio)	Vmax (PU)	Vmin (PU)
2	30	8	0.0001	0.0181	1.025	1.2	0.9104	1.05	0.95
6	31	8	0.0001	0.025	1.07	1.3	0.9554	1.05	0.965
10	32	8	0.0001	0.02	1.07	1.3	0.9554	1.05	0.95
11	12	8	0.0016	0.0435	1.006	1.2	0.8914	1.05	0.95
12	13	8	0.0016	0.0435	1.006	1.2	0.8914	1.05	0.95
19	20	8	0.0007	0.0138	1.06	1.2	0.8914	1.05	0.95
19	33	8	0.0007	0.0142	1.07	1.3	0.9554	1.05	0.95
20	34	8	0.0009	0.018	1.009	1.2	0.8944	1.05	0.95
22	35	8	0.0001	0.0143	1.025	1.2	0.914	1.05	0.95
23	36	8	0.0005	0.0272	1	1.2	0.8854	1.05	0.95
25	37	8	0.0006	0.0232	0.9938	1.2	0.8854	1.05	0.95
29	38	8	0.0008	0.0156	1.025	1.2	0.9104	1.05	0.95

4.6 EXCITATION SYSTEM AND MAXIMUM EXCITATION LIMITER DATA

The detailed modeling of the excitation system used in this thesis is explained in section Excitation System Model. The model used is ESDC1A. The dynamics data corresponding to these models are given in Table 4-7.

Table 4-7 Excitation System data

Model	KA	TA	VRMAX	VRMIN	KE	TE	KF	TF	E1	SE(E1)	E2	SE(E2)
ESDC1A	6.2	0.05	5	-5	0.5	0.05	0.06	0.1	2	0.5	4	0.9
ESDC1A	6.2	0.05	5	-5	0.5	0.05	0.06	0.1	2	0.5	4	0.9
ESDC1A	6.2	0.05	3	-3	0.5	0.05	0.06	0.1	2	0.5	4	0.9
ESDC1A	6.2	0.05	3	-3	0.5	0.05	0.06	0.1	2	0.5	4	0.9
ESDC1A	6.2	0.05	7	-7	0.5	0.05	0.06	0.1	2	0.5	5	0.6
ESDC1A	6.2	0.05	3	-3	0.5	0.05	0.06	0.1	2	0.5	4	0.9
ESDC1A	6.2	0.05	3	-3	0.5	0.05	0.06	0.1	2	0.5	4	0.9
ESDC1A	6.2	0.05	3	-3	0.5	0.05	0.06	0.1	2	0.5	4	0.9
ESDC1A	6.2	0.05	3	-3	0.5	0.05	0.06	0.1	2	0.5	4	0.9
ESDC1A	6.2	0.05	3	-3	0.5	0.05	0.06	0.1	2	0.5	4	0.9

The maximum excitation limiter model used is MAXEX1. It plays a very important role in long-term stability studies. The working principals of this model are explained in section Maximum Excitation Limiter Model. The values of the parameters are given in Table 4-8.

Table 4-8 Maximum Excitation Limiter Model data

Model	**EFD Rated**	**EFD1**	**TIME1**	**EFD2**	**TIME2**	**EFD3**	**TIME3**	**EFDDES**	**KMX**	**VLOW**
MAXEX1	3.72	0.54	20	0.57	2	0.62	1	0.3553	1	-0.3
MAXEX1	4.5	0.75	20	0.85	2	1	1	0.6202	1	-0.3
MAXEX1	3.72	0.78	20	0.8	2	0.9	1	0.6202	1	-0.3
MAXEX1	3.72	0.77	20	0.73	2	0.9	1	0.5698	1	-0.3
MAXEX1	5.289	1.4	20	1.55	2	1.65	1	0.8045	1	-0.3

Continued…

Table 4-8 Continued…

MAXEX1	3.72	0.85	20	0.9	2	0.95	1	0.6397	1	-0.3
MAXEX1	3.72	0.79	20	0.85	2	0.95	1	0.5881	1	-0.3
MAXEX1	3.72	0.71	20	0.81	2	0.9	1	0.5123	1	-0.3
MAXEX1	3.72	0.77	20	0.84	2	0.9	1	0.5636	1	-0.3
MAXEX1	3.72	0.55	20	0.65	2	0.75	1	0.3085	1	-0.3

4.7 TURBINE GOVERNOR MODEL DATA

The governor models used in this thesis are IEEEG3 and HYGOV. These are hydro governors with droop characteristics. The maximum and minimum power delivered by the governors is specified for each model. The details about the models are explained in section 3.2.4. The values of the parameters are given in Table 4-9 and Table 4-10.

Table 4-9 Turbine Governor Model data

Model	TG,	TP,	UO	UC	PMAX	PMIN	sigma	delta	TR	TW	a11	a13	a21	a23
IEEEG3	0.5	0.04	0.2	-0.1	1	0	0.05	0.3	5	3	1	1	1	1.2
IEEEG3	0.5	0.04	0.2	-0.1	1.2	0	0.05	0.3	5	3	1	1	1	1.2
IEEEG3	0.5	0.04	0.2	-0.1	1	0	0.05	0.3	5	3	1	1	1	1.2
IEEEG3	0.5	0.04	0.2	-0.1	1	0	0.05	0.3	5	3	1	1	1	1.2
IEEEG3	0.5	0.04	0.2	-0.1	1	0	0.05	0.3	5	3	1	1	1	1.2
IEEEG3	0.5	0.04	0.2	-0.1	1	0	0.05	0.3	5	3	1	1	1	1.2
IEEEG3	0.5	0.04	0.2	-0.1	1	0	0.05	0.3	5	3	1	1	1	1.2
IEEEG3	0.5	0.04	0.2	-0.1	1	0	0.05	0.3	5	3	1	1	1	1.2
IEEEG3	0.5	0.04	0.2	-0.1	1	0	0.05	0.3	5	3	1	1	1	1.2

Table 4-10 Turbine Governor Model data (2)

Model Name	R	r	Tr	Tf	Tg	VELM	GMAX	GMIN	TW	At	Dturb	qNL
HYGOV	0.05	0.5	5	0.05	0.5	0.167	1.5	0	1	1.2	1.5	0.08

Chapter 5

5 RESEARCH SIMULATIONS AND RESULTS

The proposed method of determining voltage stability using pattern recognition is tested on IEEE 39 bus system. The system is built in PSS®E. Initially, the power flow is solved to verify the validity of the data. The results are compared with other references available [40]. The standard procedure for dynamics simulation is followed and voltage stable and unstable cases are simulated by varying the load levels. Once the simulations are performed, the pattern recognition techniques are applied to extract the knowledge in the simulated data. The details are discussed in further sections.

5.1 SIMULATIONS IN PSS®E

A portion of the IEEE 39 bus system is chosen for voltage stability analysis. As per a previous study done by Beeravolu [41], bus 7 shown in the Figure 5.1 is chosen for this study. The power flow is solved for the base loading of the system as described in chapter 3. Initially, N-1 contingencies are applied to this system and it is observed that the system is well capable to handle them. The system is now stressed by increasing the real and reactive loads in steps and contingencies are applied for each loading level to observe the stability of the system. For each simulation, the following steps are followed:

1. New loading condition is created by updating the real and reactive loads
2. Power flow is solved
3. The dynamic simulation is run for 10 seconds, without any contingency
4. Contingency is applied after 10 seconds
5. The simulation is continued till 100 seconds

A python automation file is used for this purpose. We need to specify the bus number where the load is to be changed and the amount of load (P and Q) for each run.

The detailed procedure followed for the analysis is explained. First, the bus at which the load is to be increased is determined. The load (P and Q) is then increased in steps and for each step, a specific contingency is applied and the stability is observed. Once an unstable case is encountered, the details are documented. Now, we move on to the next

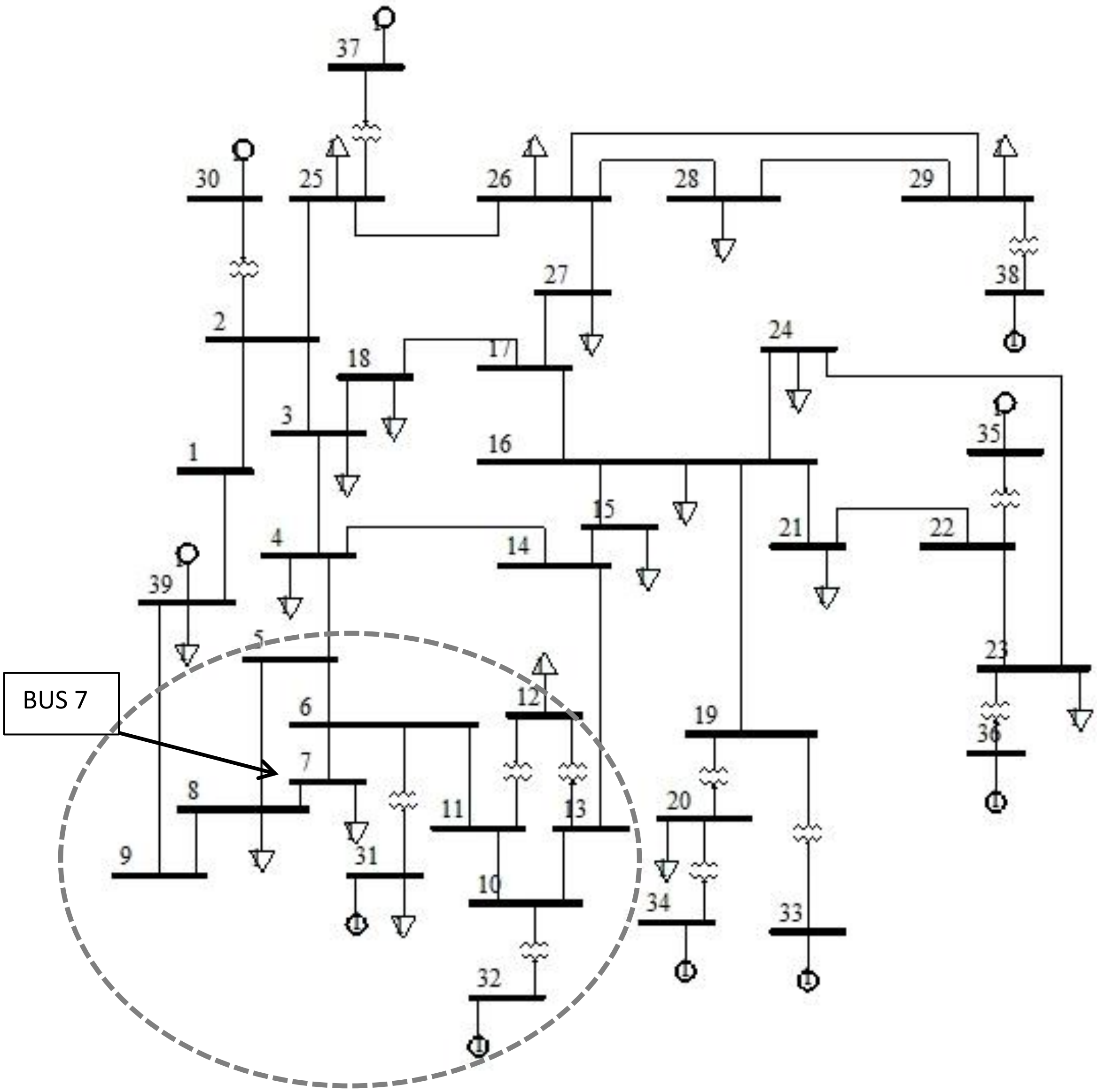

Figure 5.1 Area chosen for voltage stability analysis

contingency. All the contingencies to be applied for that bus are completed and the analysis is continued with the next bus.

The loading conditions and the corresponding contingencies applied for each training case are shown in Table 5-1.

Table 5-1 Training cases

Case #	Bus	P (MW)	Q (MW)	Contingency	Stability
1	4	600	350	Line 6 _11	Stable (+1)
2	4	550	300	Line 3_4	Stable (+1)
3	4	600	350	Line 3_4	Stable (+1)
4	4	700	450	Line 4_14	Stable (+1)
5	7	233.8	84	Line 8_9	Stable (+1)
6	7	233.8	84	Line 5_8	Stable (+1)
7	7	400	350	Line 5_8	Stable (+1)
8	7	400	250	Line 6_11	Stable (+1)
9	7	233.8	84	Line 6_11	Stable (+1)
10	8	522	176	Line 8_9	Stable (+1)
11	8	600	300	Line 8_9	Stable (+1)
12	4	700	400	Line 3_4	Unstable (-1)
13	4	750	450	Line 6_11	Unstable (-1)
14	4	750	500	Line 4_14	Unstable (-1)
15	7	400	250	Line 8_9	Unstable (-1)
16	7	500	260	Line 5_8	Unstable (-1)
17	7	450	250	Line 6_11	Unstable (-1)

The voltage magnitude plot for case 3 is shown in Figure 5.2. The load at bus 4 is increased and line 3 to 4 is disconnected after 10 seconds of dynamic simulation. Due to the loss of line 3 to 4, the voltage at bus 4 drops considerably as shown in the plot. This is due to increased reactive power demand. The terminal voltages of generators 2 and 3 are restored by the excitation control. The increased reactive power demand is supplied by these two generators. The ULTC connected between bus 6 and bus 31 (Gen 2) operates after 20 seconds and the

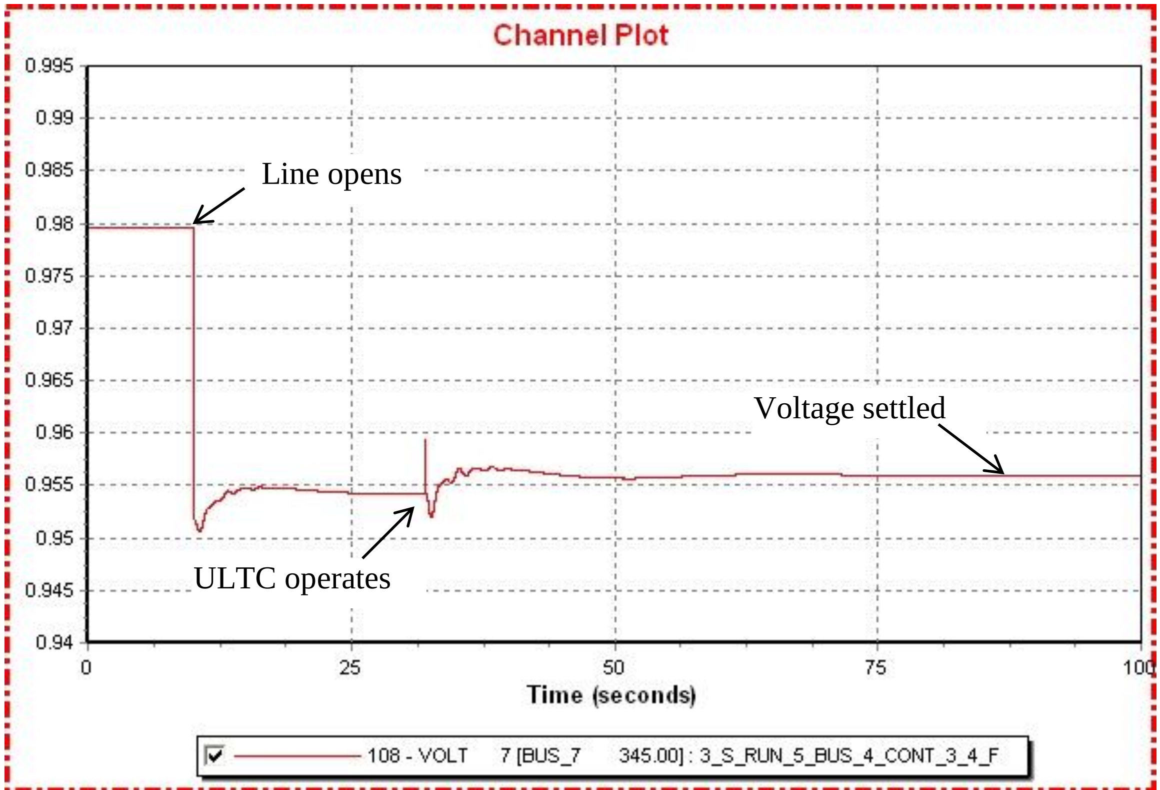

Figure 5.2 Voltage magnitude of Training case 3 - stable

voltage at controlled bus, which is bus 6 is increased. This results in an increase in the voltage level at bus 7. The voltage magnitude settles near 0.955 PU as shown in the plot.

The voltage magnitude plot of case 12 is shown in Figure 5.3. This is an unstable case. The load at bus 4 is increased, which stresses the system. After 10 seconds of simulation, the line 3 to 4 is disconnected. This results in a considerable decrease in voltage level at bus 4 due to the increased reactive power demand. The terminal voltages at generators 2 and 3 are restored by the action of excitation control. The extra reactive power is supplied by these two generators. The ULTC's connected at generators 2 and 3 restore the voltages at the controlled buses (bus 6 and bus 10). With each tap change, the line I^2X and I^2R losses increase, which in turn decrease the voltage magnitude. The reactive power output of generators throughout the system increase with each tap change. Gradually, the generators 2 and 3 reach their reactive power limits as set by their corresponding "MAXEX1" models for maximum excitation limiters. After the generators reach limits, the reactive power output is set at a constant level and the voltage finally collapses as shown in the Figure 5.3.

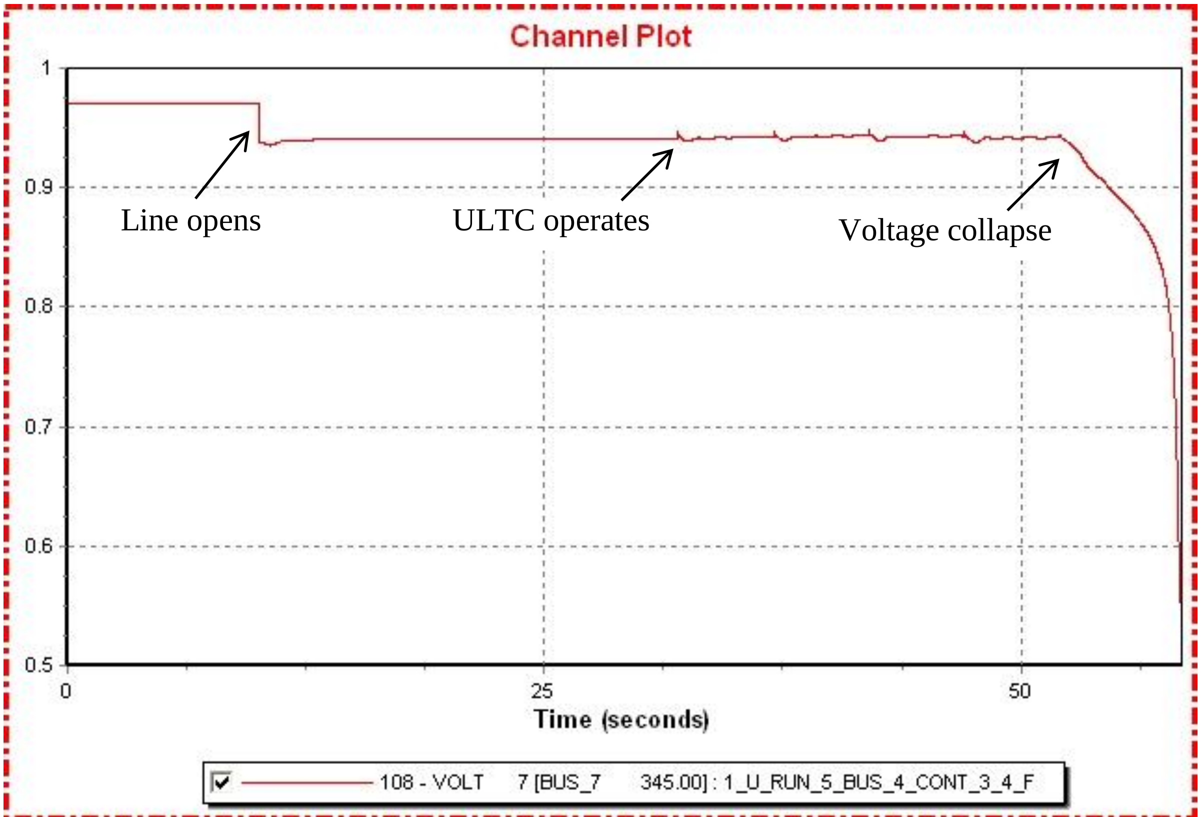

Figure 5.3 Voltage magnitude of Training Case 12 – Unstable

Table 5-2 Testing cases

Case #	Bus	P (MW)	Q (MW)	Contingency	Stability
1	8	522	176	Line 5 _8	Stable (+1)
2	8	700	450	Line 5_8	Stable (+1)
3	8	522	176	Line 6_11	Stable (+1)
4	8	650	350	Line 8_9	Unstable (-1)
5	8	700	650	Line 5_8	Unstable (-1)

The cases in Table 5-1 are used to train the RLSC algorithm and CART. Five more cases are simulated in order to test the pattern recognition model developed from the training cases. The loading conditions and the contingencies applied for each testing case are shown in Table 5-2. The same procedure described previously in this section is followed for the simulations.

5.2 REGULARIZED LEAST SQUARES METHOD

The 17 training cases shown in Table 5-1 are used to train the RLSC algorithm. The data used is voltage magnitude from 0-15 seconds, the contingency being applied after 10 seconds. Then the developed model is used to predict the stability of the testing cases shown in Table 5-2. The algorithm is implemented in MATLAB. The RLSC model made five out of five correct predictions.

Table 5-3 Results from RLSC algorithm

Case # Test	Stability Status (from simulation)	Stability Prediction (from RLSC)
1	Stable (+1)	Stable (+1)
2	Stable (+1)	Stable (+1)
3	Stable (+1)	Stable (+1)
4	Unstable (-1)	Unstable (-1)
5	Unstable (-1)	Unstable (-1)

5.3 CART

CART® is trained with the 17 training cases shown in Table 5-1. As described in section 2.5.2, raw data is not suitable for training CART; features extracted from the data are given as input to CART. The features extracted in this thesis are explained further in this section.

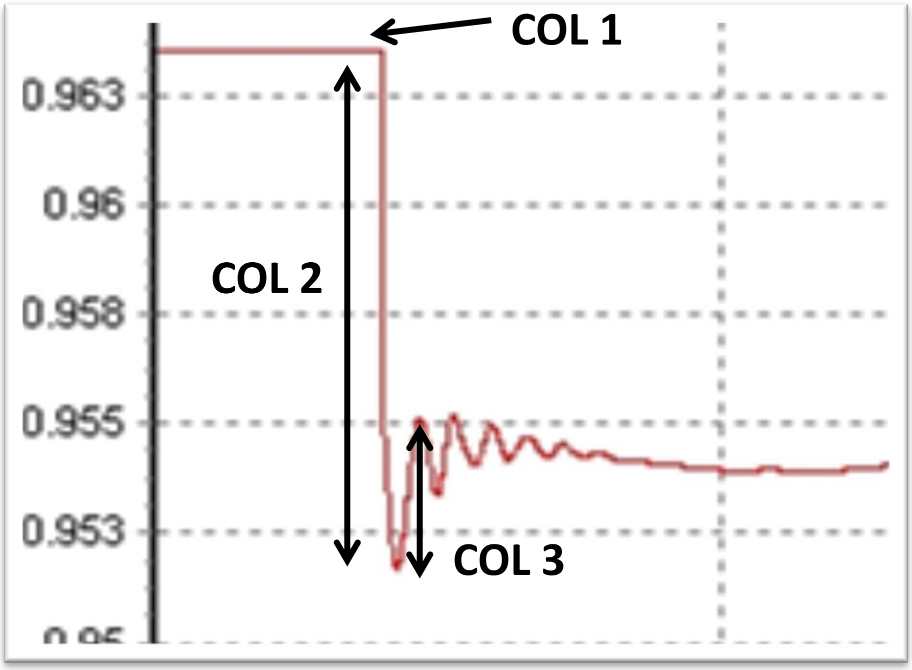

Figure 5.4 Feature 1

5.3.1 FEATURE 1

Figure 5.4 shows the feature 1 extraction from voltage magnitude cases. The data format used in CART is shown in Table 5-4. Column 1 is the value of voltage magnitude before the contingency is applied; column 2 is the magnitude of the voltage drop right after the contingency is applied, and column 3 is the magnitude of the immediate rise in voltage magnitude following the first drop. Column 4 is the ratio of the drop and rise in voltage magnitude captured previously. Column 5 is the dependent variable or prediction, +1 indicates a stable case and -1 indicates an unstable case.

Table 5-4 Feature 1 and data input format to CART

COL 1	**COL 2**	**COL 3**	**COL 4 =** COL 2/COL 3

5.3.2 FEATURE 2

Figure 5.5 shows the extraction of feature 2 from voltage magnitude cases. The contingency is applied after 10 seconds of dynamic simulation. Feature 2 is the sum of magnitudes of voltage drops and rises. The first drop as shown in the Figure 5.5 is considered to be a –ve value and the immediate rise is considered to be a +ve value. Following this trend, the drops and rises are all summed up and we get a number, which is used as feature 2.

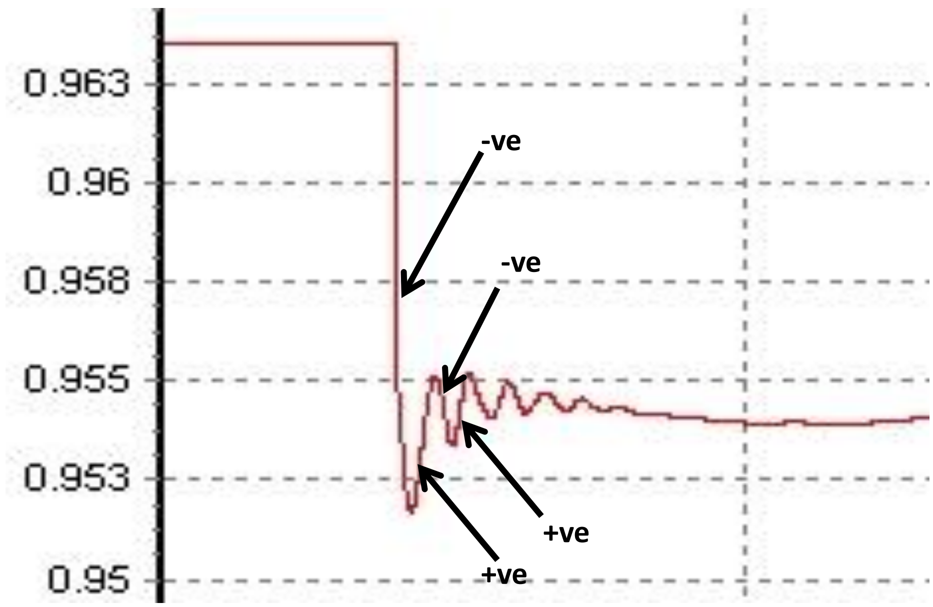

Figure 5.5 Feature 2

The data format in CART is shown in Table 5-7. COL5 refers to the 5th column in the final input given to CART which includes the features 1, 2 and 3 as explained further in this chapter.

Table 5-5 Data format for feature 2

Case #	COL 5 = sum of (-ve) drops and (+ve) rises

5.3.3 FEATURE 3

Feature 3 is essentially the same as feature 2, but the first drop in voltage magnitude when the contingency is not considered in the summation. The data format used is shown in

Table 5-6 Data input format for feature 3

Case #	**COL 6 = sum of (-ve) drops and (+ve) rises, First drop excluded**

Table 5-7 Data input format for CART

COL 1 From Feature 1	**COL2 From Feature 1**	**COL3 From Feature 1**	**COL4 From Feature 1**	**COL5 From Feature 2**	**COL6 From Feature 3**	**COL7 (Stability) +1 or -1**

5.3.4 CART TREES

The above mentioned features are extracted from the training and testing cases simulated. Matlab is used for this purpose. The training set is used to build CART trees and the input format is shown in Table 5-7. The method used is Gini index which is explained in section 2.5.2.1. Linear Combinations (LC) option is used in the analysis. LCs is all possible mathematical combinations of the variables or predictors. Instead of using a single variable for splitting a node, a linear combination of one or more predictors is used. The CART tree obtained from the training set is shown in Figure 5.6. COL1, COL2, and COL4 are the values corresponding to each case as described in Table 5-7.

The tree obtained from CART is used to predict the test cases shown in Table 5-2. The same feature is extracted from the test cases. The dependent variable or COL7 in Table 5-7 is removed. The output file created by CART is shown in Table 5-8.

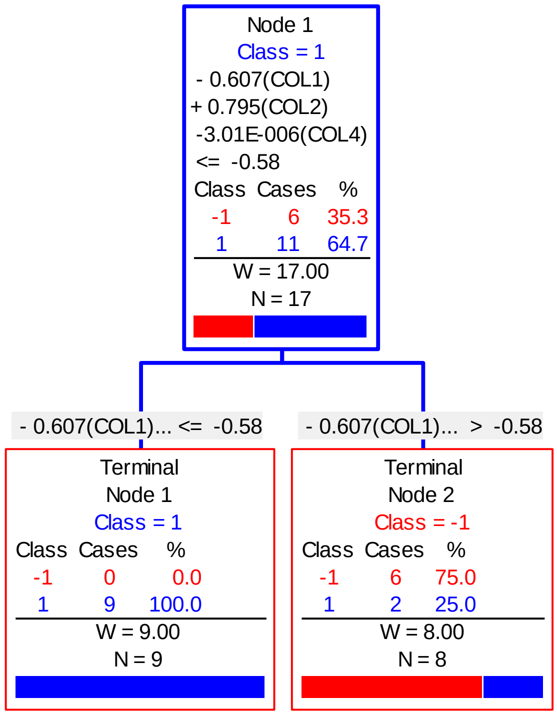

Figure 5.6 CART Tree obtained for training data using Feature 1

Table 5-8 CART output for testing cases

CASEID	RESPONSE	NODE
1	1	1
2	-1	2
3	1	1
4	-1	2
5	-1	2

Table 5-9 Results from CART

Case # Test	Stability Status (from simulation)	Stability Prediction (from CART)
1	Stable (+1)	Stable (+1)
2	Stable (+1)	Unstable (-1)
3	Stable (+1)	Stable (+1)
4	Unstable (-1)	Unstable (-1)
5	Unstable (-1)	Unstable (-1)

Test case 2 has been misclassified as unstable (-1) but it was a stable case. CART did not use the features 2 and 3 in prediction. Feature 1 is the most important feature for prediction.

Chapter 6

6 SUMMARY AND FUTURE WORK

6.1 SUMMARY

The current power grid is highly stressed due to the increased demand in electrical power without considerable addition of transmission lines. This brings a situation where the hazards of voltage collapse are highly possible to occur. This thesis presents a methodology by which we can detect the patterns in power systems which may lead to voltage collapse ahead of time. This helps the operators to take remedial actions and eventually prevent the system from collapsing. The proposed method is applied to IEEE 39 bus test system and was able to predict the voltage stability correctly. The captured dynamics of the system within 5 seconds after a contingency was used to determine and detect the patterns.

This thesis presents a review on the voltage stability analyses including the static and dynamic techniques practiced in the power systems field. The applications of pattern recognition techniques in power systems are discussed. A study of major blackouts occurred in recent times is presented. The mathematical background of power systems stability analysis is explained. Static and dynamic analyses of voltage stability are discussed. The pattern recognition techniques used in this thesis, RLSC (Regularized Least Squares Algorithm) and CART (Classification and Regression Trees) are explained in detail.

To carry on the dynamic simulations, the PSSE software is used. The static power flow analysis and dynamic analysis is done using this software. The dynamic models used in the simulation are explained in detail. The data corresponding to the IEEE 39 bus test system is presented. The complete details of all the dynamic models used are presented.

Using PSSE and the IEEE 39 bus data, a total of 22 dynamic simulations are run, out of which 17 cases are used for training the pattern recognition tools and 5 are used for testing the trained models. A small portion of IEEE 39 bus system is selected for the simulation. For each simulation, voltage at bus 7 is observed. The simulation is run for 100 seconds and the contingency is applied after 10 seconds. The data used for pattern recognition is 0-15 seconds of voltage magnitude. RLSC predicted 5 test cases correctly. CART misclassified one of the stable cases as unstable case. A final conclusion that the pattern recognition techniques can be used to predict the voltage stability ahead of time is drawn out of this thesis.

The performance of CART depends on the sample size, number of features extracted and the classifier complexity. Two main tasks involved in the analysis are feature extraction and feature selection. Feature extraction reduces the dimensionality of the problem, decreases the measurement cost, memory and increases the speed of analysis. Feature selection is the selection of best features among the extracted ones. Out of the three features extracted from the data, feature 1 came out to be the most important for prediction using CART. Features 2 and 3 are not used in the final tree CART came up with.

6.2 FUTURE WORK

The proposed methodology could be applied to large systems. For this purpose, accurate modeling of the system is necessary. On the basis of historical events, all possible critical contingencies can be prepared and the simulations can be run for these contingencies.

The proposed methodology can be used to observe the stability of entire system instead of single bus. CART and RLSC can be trained separately for different analyses such as Island detection or Angle stability. More features are to be extracted for CART, corresponding to each analysis. Measurements such as P, Q,$\angle V$, $|I|$, $\angle I$ can be included in the analysis. CART can be used in conjunction with other algorithmic approaches such as RLSC.

BIBLIOGRAPHY

[1] P. KUNDUR, Power System Stability and Control. Surrey, British Columbia: McGraw-Hill, Inc, 1994.

[2] Stephen Burnage, "The US Electric Transmission Grid: Essential infrastructure in need of comprehensive legislation," 2009.

[3] DOE, "THE SMART GRID: an introduction".

[4] IEEE/CIGRE Joint Task Force on Stability Terms and Definitions, "Definition and Classification of Power System Stability," IEEE TRANSACTIONS ON POWER SYSTEMS, vol. 19, no. 2, pp. 1387-1401, May 2004.

[5] C. W.TAYLOR, Power System Voltage Stability. Portland, Oregon: McGraw-Hill, Inc, 1994.

[6] T. Van Cutsem and R.Mailhot, "Validation of a fast voltage stability analysis method on the Hydro-Qubec System," IEEE Trans.Power Systems, vol. 12, pp. 282-292, Feb. 1997.

[7] J.D.Ainsworth, A.Gavrilovic, and H.L. Thanawala, "Static and synchronous compensators for HVDC transmission convertors connected to weak systems," 28 th session CIGRE, pp. 31-01, 1980.

[8] K.Hemmaplardh, J.W.Manke, W.R.Pauly, and J. W. Lamont, "Considerations for a Long Term Dynamic Simulation Program," IEEE Trans, vol. PWRS-1, pp. 129-135, Feb. 1986.

[9] B. Gao, G. K. Morison, and P. Kundur, "VOLTAGE STABILITY EVALUATION USING MODAL ANALYSIS," Transactions on Power Systems, vol. 7, no. 4, pp. 1529-1542, Nov. 1992.

[10] Galiana.F.D, "Load Flow Feasibility and the Voltage Collapse Problem," IEEE Proceedings of 23rd Conference on Control and Design, pp. 485-487, Dec. 1984.

[11] Tamura.Y, H.Mori, and S.Iwamoto, "Relationship between voltage instability and multiple load flow solutions in electrtic power system," IEEE Trans. on PAS, no. 5, pp. 1115-1125, May 1983.

[12] N.Yorion, et al., "AN INVESTIGATION OF VOLTAGE INSTABILITY PROBLEM," Transactions on Power Systems, vol. 7, no. 2, pp. 600-611, May

1992.

[13] Löf. P-A, Andersson. G, and Hill. D. J, "Voltage stability indices for stressed power systems," IEEE Trans. Power Systems, vol. 8, pp. 326-335, Feb. 1993.

[14] Li-Jun.C and Istavan.E, "Power System Static Voltage stability analysis considering all Active and Reactive Power Controls- singular Value approach," POWERTECH , 2007.

[15] B. H.Chowdhury and C. W.Taylor, "Voltage Stability Analysis: V –Q Power Flow Simulation Versus Dynamic Simulation ," IEEE TRANSACTIONS ON POWER SYSTEMS, vol. 15, no. 4, pp. 1354-1359, Nov. 2000.

[16] M.H.Haque and U.M.R.Pothula, "Evaluation of Dynamic Voltage Stability of a Power System," International Conference on Power System Technology - POWERCON , Nov. 2004.

[17] J.H.Chow and A.Gebreselassie, "DYNAMIC VOLTAGE STABILITY ANALYSIS OF A SINGLE MACHINE CONSTANT POWER LOAD SYSTEM," Proceedings of the 29th Conference on Decision and Control, Dec. 1990.

[18] M.Hasani and M.Parniani, "Method of Combined Static and Dynamic Analysis of Voltage Collapse in Voltage Stability Assessment," IEEE/PES Transmission and distribution Conference & Exhibition: Asia and Pacific, 2005.

[19] Zeng.Y.G, Berizzi.A, and Marannino.P, "Voltage stability analysis considering dynamic load model," Proceedings of the 4th International Conference on Advances in Power System Control, Operation and Management, APSCOM, Nov. 1997.

[20] Morison.G.K, Gao.B, and Kundar.P, "Voltage stability analysis using static anddynamic approaches," IEEE Tran. on Power Systems, vol. 8, no. 3, pp. 1159-1171, Aug. 1993.

[21] T. X. Zhu, S. K. Tso, and K. L. Lo, "An Investigation into the OLTC effects on Voltage Collapse," IEEE TRANSACTIONS ON POWER SYSTEMS, vol. 15, no. 2, pp. 515-521, May 2000.

[22] A. K. Jain, R. P. W. Duin, and J. Mao, "Statistical Pattern Recognition: A Review," IEEE TRANSACTIONS ON PATTERN RECOGNITION AND MACHINE INTELLIGENCE, vol. 22, no. 1, pp. 4-37, Jan. 2000.

[23] R. Diao, et al., "Decision Tree Assisted Controlled Islanding for Preventing Cascading Events," Power Systems Conference and Exposition, PSCE IEEE/PES,

pp. 1-8, Mar. 2009
.

[24] L. S. Moulin, A. P. A. d. Silva, M. A. El-Sharkawi, and R. J. M. II, "Support Vector Machines for Transient Stability Analysis of Large - Scale for Power Systems," IEEE TRANSACTIONS ON POWER SYSTEMS, vol. 19, no. 2, pp. 818-825, May 2004.

[25] K. Sun, S. Likhate, V. Vittal, V. S. Kolluri, and S. Mandal, "An Online Dynamic Security Assessment Scheme Using Phasor Measurements and Decision Trees," IEEE TRANSACTIONS ON POWER SYSTEMS, vol. 22, no. 4, pp. 1935-1943, Nov. 2007.

[26] L.A.Wehenkel, Automatic Learning Techniques in Power Systems. Norwell, MA: Kluwer, 1998.

[27] D.Ernst, D.R.Vega, M.Pavella, P.M.Hirsch, and D.Sobajic, "A unified approach to transient stability, contingency filtering, ranking and assessment," IEEE Trans. Power Syst.,, vol. 16, pp. 435-443, Aug. 2001.

[28] P. Zhang and J. Peng, "SVM vs Regularized Least Squares Classifications," Proceedings of the 17th International Conference on Pattern Recognition (ICPR'04), 2004.

[29] R. Diao, et al., "Decision Tree-Based Online Voltage Security Assessment Using PMU Measurements," IEEE TRANSACTIONS ON POWER SYSTEMS, vol. 24, no. 2, pp. 832-839, May 2009.

[30] I. Genc, R. Diao, and V. Vittal, "Computation of Transient Security Related Security Regions and Generation Rescheduling Based on Decision Trees," Power and Energy Society General Meeting, pp. 1-6, Jul. 2010.

[31] A. Atputharajah and T. K. Saha, "Power System Blackouts - Literature review," Fourth International Conference on Industrial and Information Systems, pp. 460-465, Dec. 2009.

[32] Ilic.M, et al., "Special issue on Power Technology and Policy: Fourty years after the 1965 Blackout," Proceedings of the IEEE, November 2005.

[33] U.S. - Canada Power System Outage Task Force;, "Final Report on the August 14, 2003 Blackout in the United States and Canada: Causes and Recomendations," April 2004.

[34] US department of Energy federal energy regulatory commission, "The Con Edison Power Failure of July 13 and 14, 1977," June 1978.

[35] Wong.C.S.M, Leevongwat.I, and Rastgoufard.P., "Angle and magnitude stability using Real-Time Simulation," Transmission and Distribution Conference and Exposition, T&D. IEEE/PES, pp. 1-4, Apr. 2008.

[36] T. Poggio and S. Smale, "The Mathematics of Learning: Dealing with Data," Notices of the American Mathematical Society (AMS), vol. 50, no. 5, pp. 537-544.

[37] B. S, Ralf.H, and Alex.S, "A generalized representer theorem," 14th Annual conference in computational learning theory, pp. 416-426, 2001.

[38] E. E. Bernabeu, "Methodology for a Security-Dependability Adaptive Protection Scheme based on Data Mining ," PhD Thesis, Virginia Polytechnic Institute and State University, 2009.

[39] Wadsworth International Group, Classification and Regression Trees. Belmont, Calif, 1984.

[40] S. Achiles, S. Schramm, and J. Bebic, "Transmission System Performance Analysis for High-Penetration Photovoltaics," National Renewable Energy Laboratory, Niskayuna, New York, Subcontract Report NRLE/SR-581-42300, 2008.

[41] N. Beeravolu, "Pattern Recognition of Power Systems Voltage Stability Using Real Time Simulations," University of New Orleans Thesis, 2010.

[42] IEEE Task Force, "Proposed Terms and Definitions for Power System Stability," vol. PAS-101, no. IEEE Trans., pp. 1894-1898, 1982.

[43] R. Sun, "VOLTAGE STABILITY INDICES BASED ON ACTIVE POWER TRANSFER USING SIMULATED PHASOR MEASUREMENTS," Clemson University A thesis , 2009.

[44] Brucoli. M. et al., "A generalized approach to the analysis of voltage stabilityin electric power systems," Proc. of Computation Conference, pp. 671-678, Sep. 1984.

[45] L. B. H and L. K. Y., "A study on voltage collapse mechanism in electric power systems," IEEE Trans. Power Systems, vol. 6, pp. 966-974, Aug. 1991.

[46] Löf. P-A, Andersson. G, and Hill D. J., "Voltage dependent reactive power limits for voltage stability studies," IEEE Trans. Power Systems, vol. 8, pp. 220-228, Feb. 1995.

[47] Van Cutsem.T and et.al., "A comprehensive analysis of mid-term voltage stability," IEEE Transactions on Power Systems, vol. 3, no. 4, pp. 1173-1182, Aug.

1995.

[48] Ajjarapu.V and Christy.C, "The continuation power flow: A tool for steady state voltage stability analysis," IEEE Trans. on Power Systems, vol. 7, no. 1, pp. 416-423, Feb. 1992.

[49] Begovic.M.M and Phadke.A.G., "Control of voltage stability using sensitivity analysis," IEEE Transactions on Power Systems, vol. 7, no. 1, pp. 114-123, Feb. 1992.

[50] DeMarco.C.L and Overbye.T.J., "Improved techniques for power systen voltage stability assessment using energy methods.," IEEE Transactions on Power Systems, vol. 6, no. 4, pp. 1446-1452, Nov. 1991.

[51] Huang.G and Zhu.T, "A new method to find the voltage collapse point," Proc. of Power Engineering Society Winter Meeting IEEE, vol. 2, pp. 1324-1329, Jul. 1999.

[52] W. C. S. M, Rastgoufard.P, and M. D, "Voltage Stability Studies Using Real-Time Simulation Computing," System Theory, 40th south eastern symposium, pp. 410-414, Mar. 2008.

[53] H.-D. Chiang, I. Dobson, Robert.J.Thomas, James.S.Thorp, and F. Ahmed, "On Voltage Collapse in Electric Power Systems," IEEE Transactions on Power Systems, vol. 5, no. 2, pp. 601-611, May 1990.

[54] R. Sun, "VOLTAGE STABILITY INDICES BASED ON ACTIVE POWER TRANSFER USING SIMULATED PHASOR MEASUREMENTS," Clemson University Thesis, 2009.

[55] R. M. Rifkin, "Everything Old Is New Again: A Fresh look at Historical Approaches in Machine Learning," MASSACHUSETTS INSTITUTE OF TECHNOLOGY, 2002.

[56] Siemens PTI. (2010, Oct.) Siemens PTI, PSS®E Online Documentation.

[57] J. Bian, P. Rastgoufard, and J. Davey, "TRANSMISSION SYSTEM RELIABILITY ANALYSIS IN POWER SYSTEMS RELIABILITY INSTRUCTION," System Theory Proceedings, pp. 213-216, 1992.

VITA

The author was born in 1987, in India. He completed his bachelors of engineering degree in Electrical and Electronics Engineering from Osmania University, Hyderabad India in 2009. He finished his Masters in Electrical Engineering from the University of New Orleans in May 2012. He worked as a Research Assistant with Dr. Parviz Rastgoufard during Masters. His areas of interests are dynamic simulation studies, modeling of power systems, voltage stability analyses.